



**Pronounced Antibacterial Effects of Rhodomyrtone, a Novel
Antibiotic Candidate, on *Streptococcus pneumoniae* as Revealed by
Proteomic and Metabolomic Analysis**

Watcharapong Mitsuwan

**A Thesis Submitted in Fulfillment of the Requirements for the
Degree of Doctor of Philosophy in Microbiology**

Prince of Songkla University

2019

Copyright of Prince of Songkla University



**Pronounced Antibacterial Effects of Rhodomyrtone, a Novel
Antibiotic Candidate, on *Streptococcus pneumoniae* as Revealed by
Proteomic and Metabolomic Analysis**

Watcharapong Mitsuwan

**A Thesis Submitted in Fulfillment of the Requirements for the
Degree of Doctor of Philosophy in Microbiology**

Prince of Songkla University

2019

Copyright of Prince of Songkla University

Thesis Title Pronounced Antibacterial Effects of Rhodomyrtone, a Novel Antibiotic Candidate, on *Streptococcus pneumoniae* as Revealed by Proteomic and Metabolomic Analysis

Author Mr. Watcharapong Mitsuwan

Major Program Microbiology

Major Advisor

.....
(Prof. Dr. Supayang Voravuthikunchai)

Examining Committee:

.....Chairperson
(Asst. Prof. Dr. Potjanee Srimanote)

Co-advisor

.....
(Prof. Dr. Manuel J. Rodríguez-Ortega)

..... Committee
(Prof. Dr. Supayang Voravuthikunchai)

.....Committee
(Dr. Jongkon Saising)

..... Committee
(Dr. Wipawadee Sianglum)

The Graduate School, Prince of Songkla University, has approved this thesis as fulfillment of the requirements for the Doctor of Philosophy Degree in Microbiology

.....
(Prof. Dr. Damrongsak Faroongsarng)

Dean of Graduate School

This is to certify that the work here submitted is the result of the candidate's own investigations. Due acknowledgement has been made of any assistance received.

.....Signature
(Prof. Dr. Supayang Voravuthikunchai)
Major Advisor

.....Signature
(Mr. Watcharapong Mitsuwan)
Candidate

I hereby certify that this work has not been accepted in substance for any degree, and is not being currently submitted in candidature for any degree.

.....Signature
(Mr. Watcharapong Mitsuwan)
Candidate

Thesis Title	Pronounced antibacterial effects of rhodomyrtone, a novel antibiotic candidate, on <i>Streptococcus pneumoniae</i> as revealed by proteomic and metabolomic analysis
Author	Mr. Watcharapong Mitsuwan
Major Program	Microbiology
Academic Year	2018

ABSTRACT

The emergence of antibiotic-resistant pathogenic bacteria is a healthcare problem worldwide. We evaluated the antimicrobial activity of rhodomyrtone, an acylphloroglucinol present in *Rhodomyrtus tomentosa* leaves, against the human Gram-positive pathogens, *Streptococcus pneumoniae*. The compound exhibited pronounced anti-pneumococcal activity against a broad collection of clinical isolates. We studied the effects at the molecular level by a combination of proteomics and metabolomics. The integration of proteomic and metabolomic analyses revealed alterations in enzymes and metabolites involved in different metabolic pathways including amino acid biosynthesis, nucleic acid biosynthesis, glucid, and lipid metabolism. Notably, the levels of two enzymes (glycosyltransferase and UTP-glucose-1-phosphate uridylyltransferase) and three metabolites (UDP-glucose, UDP-glucuronic acid and UDP-N-acetyl-D-galactosamine) participating in the synthesis of the pneumococcal capsule clearly diminished in cells exposed to rhodomyrtone. Rhodomyrtone-treated pneumococcal cells significantly possessed less amount of capsule, as measured by a colorimetric assay and visualized by electron microscopy. These findings reveal the utility of combining proteomic and metabolomic analyses to provide insight into phenotypic features of *S. pneumoniae* treated with this potential novel antibiotic.

The ability of *Rhodomyrtus tomentosa* leaf extract and rhodomyrtone to prevent biofilm formation and eradicate mature biofilms was assessed. The extract and rhodomyrtone at $1/8 \times \text{MIC}$ significantly inhibited biofilm formation in all clinical isolates ($P < 0.05$). The viability of 8-day biofilm-grown cells significantly decreased following the treatment with the extract and rhodomyrtone at $16 \times \text{MIC}$. 40-90% reduction in the bacterial adhesion and invasion to A549 human alveolar epithelial cells was observed after challenging with the extract and rhodomyrtone, compared with the

control within 60 min. Increase in 90-99% phagocytosis of the bacterial cells by RAW264.7 macrophage cell line was detected following the treatment with the extract and rhodomyrtone at $1/2 \times \text{MIC}$, compared with the control. The results suggested potential medicinal benefits of the extract and rhodomyrtone for the treatment of pneumococcal infections.

In conclusion, rhodomyrtone is a promising alternative antibacterial agent for the treatment of the infections caused by the Gram-positive pathogens including *S. pneumoniae*.

Key words: Rhodomyrtone, *Rhodomyrtus tomentosa*, *Streptococcus pneumoniae*, proteomic, metabolomic

ชื่อวิทยานิพนธ์ ฤทธิ์การยับยั้งแบคทีเรีย *Streptococcus pneumoniae* ของโรโดไมรโทน โดยการ
วิเคราะห์ทางโปรติโอมิกส์และเมตาโบโลมิกส์

ผู้เขียน นายวัชรพงษ์ มิตสุวรรณ

สาขาวิชา จุลชีววิทยา

ปีการศึกษา 2561

บทคัดย่อ

อุบัติการณ์เชื้อแบคทีเรียคือยาปฏิชีวนะเป็นปัญหาสำคัญทั่วโลก งานวิจัยนี้ศึกษาฤทธิ์ของสารโรโดไมรโทนซึ่งเป็นกลุ่ม acylphloroglucinol แยกจากใบปกระทุงในการต้านเชื้อแบคทีเรียก่อโรคร่วมพวก *Streptococcus pneumoniae* สารโรโดไมรโทนมีฤทธิ์ต้านเชื้อแบคทีเรีย *S. pneumoniae* ที่แยกได้จากผู้ป่วย ศึกษาฤทธิ์ของโรโดไมรโทนในระดับโมเลกุลโดยวิธีโปรติโอมิกส์และเมตาโบโลมิกส์ พบว่ามีการเปลี่ยนแปลงของเอนไซม์และสารเมทาบอลิท์ที่เกี่ยวข้องกับกระบวนการเมทาบอลิซึมของการสังเคราะห์กรดอะมิโน กรดนิวคลีอิก คาร์โบไฮเดรต และไขมัน ของเชื้อ *S. pneumoniae* ในสถานะที่มีสารโรโดไมรโทน เป็นที่น่าสังเกตว่าระดับของเอนไซม์ glycosyltransferase และ UTP-glucose-1-phosphate uridylyltransferase และสารเมทาบอลิท์ประกอบด้วย UDP-glucose, UDP-glucuronic acid และ UDP-N-acetyl-D-galactosamine ลดลงในสถานะที่มีสารโรโดไมรโทน โดยเอนไซม์และสารดังกล่าวเกี่ยวข้องกับกระบวนการสังเคราะห์แคปซูลของเชื้อ *S. pneumoniae* สารโรโดไมรโทนลดการสังเคราะห์แคปซูลของเชื้อ *S. pneumoniae* ซึ่งศึกษาด้วยการวัดปริมาณแคปซูลและภาพถ่ายอิเล็กตรอนชนิดส่องผ่าน

สารสกัดใบกระทุงที่สกัดด้วยเอทานอล และสารบริสุทธิ์โรโดไมรโทนที่ความเข้มข้น $1/18 \times$ MIC ยับยั้งการสร้างไบโอฟิล์มของเชื้อ *S. pneumoniae* ที่แยกได้จากผู้ป่วย อย่างมีนัยสำคัญ สารสกัดใบกระทุงและโรโดไมรโทนที่ความเข้มข้น $16 \times$ MIC ฆ่าเชื้อในไบโอฟิล์มที่มีอายุ 8 วัน อย่างมีนัยสำคัญ สารสกัดใบกระทุงและโรโดไมรโทนลดการเกาะติดและการบุกรุกของเชื้อ *S. pneumoniae* ต่อ A549 human alveolar epithelial cells

ภายในเวลา 60 นาที เชื้อ *S. pneumoniae* ที่เลี้ยงในสภาวะที่มีสารสกัดใบกระทุงและโรโดไมรโทนถูกจับกินโดย RAW264.7 macrophage cell line เพิ่มขึ้น 90-99% เมื่อเทียบกับชุดควบคุม จากผลการทดลองที่กล่าวมาแสดงให้เห็นถึงศักยภาพของสารโรโดไมรโทนในการยับยั้งเชื้อ *S. pneumoniae*

โดยสรุป rhodomyrton เป็นสารต้านแบคทีเรียทางเลือกที่มีแนวโน้มสำหรับการรักษาโรคติดเชื้อที่เกิดจากเชื้อกรัมบวกที่มีสาเหตุจากเชื้อ *S. pneumoniae*

ACKNOWLEDGMENTS

I would like to express my sincere grateful thanks and sincere appreciation to my advisor, Professor Dr. Supayang Voravuthikunchai, for her helpful suggestion, valuable guidance and comments throughout my study. Sincere appreciation is expended to Professor Dr. Manuel J. Rodríguez-Ortega, my co-advisor, for his valuable contribution and advice relating to this study.

I would like to thank examining committees, Assistant Professor Dr. Potjane Srimanote, Dr. Jongkon Saising, and Dr. Wipawadee Sianglum, for their constructive comments and suggestion on my thesis.

I wish to express my gratitude to The Thailand Research Fund (TRF) through the Royal Golden Jubilee (RGJ) Ph.D. Program, grant number; PHD/0053/2553, which support my work and by the Graduate School, Prince of Songkla University is also acknowledged for partly supported to establish this work.

I would like to thank Dr. Alfonso Olaya-Abril and Dr. Irene Jiménez-Munguía for their suggestions and assistance in part of multi-omics.

I would like to express my beloved friends and staffs at Natural Product Research Center of Excellence for their kindly and helpful advice during my entire study.

Finally, I wish to thanks my beloved, father, mother, including my brother and all best friends for their supporting and encouragement.

Watcharapong Mitsuwan

CONTENTS

	Page
Abstract	v
Abstract (in Thai)	vii
Acknowledgment	ix
List of Tables	xii
List of Figures	xiii
List of Abbreviations	xv
CHAPTER 1 Introduction	1
Rationale and Background	1
Literature Reviews	4
Research objectives	20
CHAPTER 2 Research Methodology	21
Antibacterial agents	21
Bacterial strains and growth conditions	21
Cell culture	21
Determination of minimal inhibitory concentration and minimal bactericidal concentration	22
Time-kill study	22
Preparation of cellular and secreted proteins	22
Two-dimensional gel electrophoresis (2DE)	23
Protein identification by MALDI-TOF/TOF MS	24
Preparation of metabolite extracts	25
Metabolite identification by LC-MS/MS	25
Quantification of capsule	26
Transmission electron microscopy	27
Phagocytosis of <i>Streptococcus pneumoniae</i> treated with sub-MICs of the extract and rhodomyrtone	27
Effects of <i>Rhodomyrtus tomentosa</i> ethanol extract and rhodomyrtone on <i>Streptococcus pneumoniae</i> biofilm formation	28

CONTENTS (Continued)

	Page
Effects of <i>Rhodomyrtus tomentosa</i> ethanol extract and rhodomyrtone on <i>Streptococcus pneumoniae</i> established biofilm	28
Effects of <i>Rhodomyrtus tomentosa</i> extract and rhodomyrtone on pneumococcal adhesion and invasion to A549 human lung adenocarcinoma cell line	29
Statistical analysis	29
CHAPTER 3 Results	30
<i>In vitro</i> antibacterial activity of <i>Rhodomyrtus tomentosa</i> ethanol extract and rhodomyrtone against clinical isolates of <i>S. pneumoniae</i>	30
Time-kill study	32
Effects of purified rhodomyrtone on the pneumococcal growth	36
Effects of purified rhodomyrtone on the pneumococcal proteome	38
Effects of purified rhodomyrtone on the pneumococcal metabolome	45
Effect of purified rhodomyrtone on the pneumococcal capsule	53
Phagocytosis of <i>S. pneumoniae</i> treated with sub-MICs of the extract and rhodomyrtone	56
<i>Rhodomyrtus tomentosa</i> leaf ethanol extract and rhodomyrtone inhibit biofilm formation in <i>S. pneumoniae</i>	59
Killing effects of <i>Rhodomyrtus tomentosa</i> ethanol extract and rhodomyrtone on pneumococcal established biofilm	62
Effects of <i>Rhodomyrtus tomentosa</i> extract and rhodomyrtone on pneumococcal adhesion and invasion to A549 human lung adenocarcinoma cell line	65
CHAPTER 4 Discussion	68
CHAPTER 5 Conclusion	76
References	77
Vitae	93

LIST OF TABLES

Table	Page
1. Mechanism of antibiotic resistance in <i>S. pneumoniae</i>	12
2. Minimal inhibitory concentration (MIC) and minimal bactericidal concentration (MBC) values of <i>Rhodomyrtus tomentosa</i> ethanol extract, purified rhodomyrtone, and synthetic rhodomyrtone against <i>Streptococcus pneumoniae</i> clinical isolates	31
3. Cellular proteins altered after purified rhodomyrtone treatment of <i>Streptococcus pneumoniae</i>	42
4. Secreted proteins altered after purified rhodomyrtone treatment of <i>Streptococcus pneumoniae</i>	44
5. Metabolites altered after rhodomyrtone treatment of <i>Streptococcus pneumoniae</i>	47

LIST OF FIGURES

Figure	Page
1. Image of <i>Rhodomyrtus tomentosa</i> (Aiton) Hassk.	16
2. Structure of rhodomyrtone	18
3. Research representation of rhodomyrtone study	19
4. Time-kill curves of <i>S. pneumoniae</i> TIGR4, R6, and 5335-5 after treatment with <i>Rhodomyrtus tomentosa</i> ethanol extract	33
5. Time-kill curves of <i>S. pneumoniae</i> TIGR4, R6, and 5335-5 after treatment with purified rhodomyrtone	34
6. Time-kill curves of <i>S. pneumoniae</i> TIGR4, R6, and 5335-5 after treatment with synthetic rhodomyrtone	35
7. Growth curves of <i>Streptococcus pneumoniae</i> in the presence or absence of rhodomyrtone	37
8. Representative 2-D gels of cellular proteins of <i>S. pneumoniae</i> TIGR4 and R6 cultured with $1/2 \times$ MIC purified rhodomyrtone	40
9. Representative 2-D gels of secreted proteins of <i>S. pneumoniae</i> TIGR4 and R6 cultured with $1/2 \times$ MIC purified rhodomyrtone	41
10. Principal component analysis of the metabolite profile of <i>S. pneumoniae</i> treated with $1/2 \times$ MIC rhodomyrtone	46
11. Inhibition of pneumococcal capsule by purified rhodomyrtone	54
12. Capsular illustration by transmission electron microscopy of <i>S. pneumoniae</i> TIGR4 cells before and after exposure to $1/2 \times$ MIC purified rhodomyrtone	55
13. Activity of <i>Rhodomyrtus tomentosa</i> ethanol extract on phagocytosis of <i>S. pneumoniae</i> NPRCoE 16507 and ATCC 49619	57
14. Activity of rhodomyrtone on phagocytosis of <i>S. pneumoniae</i> NPRCoE 16507 and ATCC 49619	58
15. Effects of <i>Rhodomyrtus tomentosa</i> ethanol extract on <i>Streptococcus pneumoniae</i> growth and biofilm formation	60

LIST OF FIGURES

Figure	Page
16. Effects of rhodomyrtone on <i>Streptococcus pneumoniae</i> growth and biofilm formation	61
17. Inhibitory activity of <i>Rhodomyrtus tomentosa</i> ethanol extract on established biofilm of <i>Streptococcus pneumoniae</i>	63
18. Inhibitory activity of rhodomyrtone on established biofilm rhodomyrtone on established biofilm of <i>Streptococcus pneumoniae</i>	64
19. Effects of <i>Rhodomyrtus tomentosa</i> ethanol extract and rhodomyrtone on <i>Streptococcus pneumoniae</i> adhesion	66
20. Effects of <i>Rhodomyrtus tomentosa</i> ethanol extract and rhodomyrtone on <i>Streptococcus pneumoniae</i> invasion	67

LIST OF ABBREVIATIONS

ATCC	=	American Type Culture Collection
BHI	=	Brain heart infusion
CO ₂	=	Carbon dioxide
CFU	=	Colony forming unit
DMEM	=	Dulbecco's Modified Eagle Medium
° C	=	Degree Celsius
DMSO	=	Dimethyl sulfoxide
MTT	=	3-(4, 5-dimethylthiazol-2-yl)-2, 5- diphenyltetrazolium bromide
FBS	=	Fetal bovine serum
h	=	Hour
MV	=	Membrane vesicle
µg	=	Microgram
µl	=	Microlite

LIST OF ABBREVIATIONS (Continued)

MBC	=	Minimal bactericidal concentration
MIC	=	Minimal inhibitory concentration
MHB	=	Mueller Hinton Broth
PBS	=	Phosphate-buffered saline
%	=	Percent
RPMI1640	=	Roswell Park Memorial Institute
THB	=	Todd Hewitt broth
TSA	=	Trypticase soy aga

CHAPTER 1

INTRODUCTION

1.1 Rationale and Background

Streptococcus pneumoniae (pneumococcus) infections are an important cause of morbidity and mortality in humans including infants and older adults. Actually, it is estimated that around three million children <5 years die every year because of pneumococcal disease, mainly in developing countries (Farooqui, Jit et al. 2015). The bacterium colonizes in the human upper respiratory tract including nasopharynx. Colonization is a prerequisite for subsequent spread, which may result in pneumococcal infections including community-acquired pneumonia, otitis media, bronchitis, sinusitis, meningitis, and septicemia. The organism is the most common cause of community-acquired pneumonia leading to morbidity and mortality in infants and older adults (van der Poll and Opal 2009). In addition, *S. pneumoniae* is one of the most important pathogens in otitis media. It has been reported that *S. pneumoniae* serotype 19A ST320 is the predominant cause of pneumococcal mastoiditis, a suppurative complication of acute otitis media (Chi, Chiu et al. 2018).

Virulence factors produced by *S. pneumoniae* play an important role against host defense. The initial phase of pathogenesis of the pathogen is associated with attachment, colonization, followed by invasion. During nasopharyngeal colonization, the organism produces biofilm structures that develops into complex structures. The bacterial biofilms are detected on mucosal surfaces during pneumonia and middle ear infection (Chao, Marks et al. 2015). Biofilms play an important role in the pathogenesis of the infection, and are associated with antibiotic resistance. The pathogen produces a protective surface structure known as capsule that is considered as the main virulence factor (James, Gupta et al. 2013, Wen, Liu et al. 2016, Wu, Xu et al. 2016). The capsule contributes in invasive infection, inhibition of phagocytosis, and prevention of complement disposition (Hyams, Camberlein et al. 2010). Therefore, biofilm formation and capsule polysaccharide in pneumococci are a potent strategy to evade host immune system including phagocytosis (Domenech, Ramos-Sevillano et al.

2013). Nowadays, treatment of *S. pneumoniae* infections is becoming difficult due to the increase in antibiotic resistance of the organism (Cai, Wang et al. 2018).

There is a high demand to find novel antibacterial agents to overcome antibiotic resistant pathogens. Medicinal plants have been used to treat the bacterial infections due to the activities of their secondary metabolites. *Rhodomyrtus tomentosa* (Aiton) Hassk. is a flowering medicinal plant that belongs to the family Myrtaceae. Previous studies of our research group have reported that *Rhodomyrtus tomentosa* ethanol extract possesses strong antibacterial activity against a wide range of Gram-positive pathogens including *Bacillus cereus*, *Enterococcus faecalis*, *Listeria monocytogenes*, *Staphylococcus aureus*, *S. mutans*, *S. pneumoniae*, and *S. pyogenes* (Limsuwan, Trip et al. 2009). Interestingly, rhodomyrtone, an acylphloroglucinol derivative isolated from *Rhodomyrtus tomentosa* leaves, has shown pronounced antibacterial activity against important human pathogens including *S. pneumoniae* capsule-producing strain (Limsuwan, Trip et al. 2009).

The effects of rhodomyrtone at molecular level have been studied in a few Gram-positive species including *S. aureus* (Sianglum, Srimanote et al. 2011) and *S. pyogenes* (Limsuwan, Hesseling-Meinders et al. 2011). Proteomic analysis has revealed that rhodomyrtone affected the expression of several major classes of cellular proteins in methicillin-resistant *S. aureus* (MRSA) (Sianglum, Srimanote et al. 2011). In addition, transcriptome analysis has revealed that rhodomyrtone caused a significant modulation of gene expression, with induction of 64 genes and repression of 35 genes in MRSA (Sianglum, Srimanote et al. 2012). Proteomic analysis of rhodomyrtone-treated *S. pyogenes* has shown that the compound affects the expression of streptococcal secreted and whole cell proteins (Limsuwan, Hesseling-Meinders et al. 2011). The altered proteins were identified as enzymes associated with important pathways of the primary metabolism (Limsuwan, Hesseling-Meinders et al. 2011). It has been reported that rhodomyrtone caused large membrane invaginations with an increase in fluidity. It has been documented that rhodomyrtone transiently binds to phospholipid head groups and causes distortion of lipid packing, providing explanations for membrane fluidization and induction of membrane curvature as revealed by molecular dynamics simulation analysis. It has been reported that both its transient binding mode and its

ability to form protein-trapping membrane vesicles are unique, making it an attractive new antibiotic candidate with a novel mechanism of action (Saeloh, Tipmanee et al. 2018). However, deep detail mechanisms of rhodomyrtone on the inhibition of the bacterial virulence factors which play important roles in infection are needed to be investigated. In addition, pharmacokinetic and pharmacodynamic of rhodomyrtone on animal models have not been widely studied.

Novel genome analysis approaches including proteome, transcriptome, and metabolome analysis have become an effective machinery to investigate mutations linked to drug resistance or antibiotic mode of action. Proteome analysis are high throughput analytical methods for study of the cellular function (Rogers, *et al.*, 2007). Metabolome analysis covers the identification and quantification of all intracellular and extracellular metabolites using various analytical approaches. The metabolome includes considerably different chemical components including carbohydrates, volatile alcohols and ketones, amino and non-amino organic acids, hydrophobic lipids (Liebeke, *et al.*, 2012).

The aim of this study was to investigate the antibacterial effects of rhodomyrtone on *S. pneumoniae*, and the changes induced at molecular level using proteomics and metabolomics. We have studied the response of two reference pneumococcal strains including the virulence, encapsulated strain TIGR4 and the non-encapsulated avirulent strain R6 in the presence of the purified compound, using proteomics and metabolomics. The effects of *Rhodomyrtus tomentosa* leaf extract and rhodomyrtone were further determined on *S. pneumoniae* virulence factors including biofilms, capsule formation, and invasiveness which play important roles in infections.

1.2 Literature Reviews

1.2.1 *Streptococcus pneumoniae*

Streptococcus pneumoniae, belonging to family Streptococcaceae, is microaerophilic, Gram-positive diplococci. The bacterium appears as lancet-shaped when viewed through a microscope. A single cell or chains are also seen in sputum or pus. The bacterium is non-endospore-forming and non-motile. *S. pneumoniae* forms tiny round colonies which occurred dome shaped. The pneumococci typically possess α -haemolysis with green discoloration of agar around the colonies on blood agar. The optimal growth condition is 37 °C with 5-10% CO₂. *S. pneumoniae* produces capsule which protects them from phagocytosis by polymorphonuclear leukocytes. The polysaccharide capsule is the most important virulence factor of the organism (Peppoloni, Ricci et al. 2010).

S. pneumoniae asymptotically colonizes the upper respiratory tract of human. Under appropriate conditions, this microorganism may become a leading cause of serious diseases including community acquired pneumonia, otitis media, sinusitis, meningitis, empyema, septic arthritis, endophthalmitis, and septicemia. The organism is the most common cause of community-acquired pneumonia leading to morbidity and mortality in infants and older adults (van der Poll and Opal 2009). *S. pneumoniae* is one of important pathogens in otitis media. It has been reported that *S. pneumoniae* serotype 19A ST320 is the predominant cause of pneumococcal mastoiditis, a suppurative complication of acute otitis media (Chi, Chiu et al. 2018). The large burden of disease, causes by the pathogen is compounded by an increased incidence of the pneumococcal infections associated with HIV and immunocompromised patients and by increasing antibiotic resistance among clinical isolates (Cillóniz, García-Vidal et al. 2018).

1.2.2 Virulence factors of *S. pneumoniae*

1.2.2.1 Polysaccharide capsule

The organism can be characterized into over 90 serotypes according to the composition of their polysaccharide capsules (Hathaway, Grandgirard et al. 2016). The reaction between the polysaccharide capsule and specific antibody is classified serotypes of *S. pneumoniae*. Pneumococcal capsule synthesis occurs by one of two

distinct mechanisms including Wzy dependent and synthase dependent mechanism. The mechanisms involve the polymerization of either individual sugars in a processive reaction (synthase dependent) or discrete repeat units in a nonprocessive reaction (Wzy dependent) (Yother 2011). The enzymes necessary for the polysaccharide synthesis are encoded within the polysaccharide-specific loci. The polysaccharide capsule operon (Wzy dependent mechanism) is flanked by the genes *dexB* and *aliA*. The locus contains four conserved sequences including *cpsA* (*wzg*), *cpsB* (*wzh*), *cpsC* (*wzd*), and *cpsD* (*wze*). This locus is important in the modulation of capsule synthesis in the serotypes, except serotypes 3 and 37 (Kurola, Erkkilä et al. 2010). The next gene encodes the initiating glycosyltransferase. Diphospho-sugars (NDP-sugars) are common substrate of capsule repeating units. The common precursors include UDP-Glc, UDP-GlcNAc (peptidoglycan, teichoic acids), UDP-galactose (lipopolysaccharide), and UDP-N-acetylgalactosamine (teichoic acids) (Yother 2011). Synthase-dependent mechanism is simpler than Wzy-dependent mechanism. It usually consists of only one or two sugars. The polysaccharide may be linear or branched by the linkage catalyzed by the synthase during polymerization of sugars. Synthase-dependent mechanism is important in the modulation of capsule synthesis in the serotypes 3 and 37 (Yother 2011).

Capsule formation is considered as one among the vital pathogenic factor that contributes in invasive infection, inhibition of phagocytosis, and prevention of complement disposition (Hyams, Camberlein et al. 2010). Transparent strains are more efficient in colonizing the mucosal surface of the nasopharynx. On the other hand, the opaque strains are more virulent than the transparent strains in systemic infections (Kurola, Erkkilä et al. 2010).

1.2.2.2 Pneumococcal biofilm

S. pneumoniae is present in the human upper respiratory tract as a colonizer. Under appropriate conditions, this microorganism may become a leading cause of serious diseases. The initial phase of pathogenesis of the bacteria is associated with attachment, colonization, followed by invasion. During nasopharyngeal colonization, the bacterium produces biofilm structures that develops into complex structures. Biofilms are highly-structured communities of cells that produce an extracellular matrix and adhere to surfaces. Pneumococcal biofilms are detected on

mucosal surfaces during pneumonia and middle ear infection (Chao, Marks et al. 2015). The biofilms play an important role in the pathogenesis of the infection, and are associated with antibiotic resistance. Biofilm formation in pneumococci are a potent strategy to evade host immune system including phagocytosis (Domenech, Ramos-Sevillano et al. 2013). Furthermore, treatment of pneumococcal infections is becoming difficult due to the increase in antibiotic resistance of the organism.

It has been reported that the bacterial biofilm is controlled by quorum sensing system (Solano, Echeverz et al. 2014). Quorum sensing is a bacterial cell to cell communication that synchronizes bacterial gene expression in response to cell density. Quorum sensing regulates bacterial virulence factors including the biofilm by production and sensing of pheromone called autoinducer. It has been reported that Rgg/ small hydrophobic peptide (SHP) quorum-sensing systems are widespread in streptococci including *S. pneumoniae* (Junges, Salvadori et al. 2017). Small hydrophobic peptide acts as an autoinducer via Rgg. Rgg/small hydrophobic peptide complexes activate transcription by binding to the promoter sites resulting in biofilm formation. It has been reported that an expression of both *shp* and *rgg* genes increased at the stationary growth phase of *S. pneumoniae* (Junges, Salvadori et al. 2017). It has been reported that arginine deiminase system protects bacterial cells against damaging effects of acid environments (Casiano-Colón and Marquis 1988). Carbohydrate fermentation by bacteria embedded in the biofilm generates acidic metabolites. Arginine deiminase generates L-citrulline and ammonia from L-arginine. The produced ammonia could neutralize acid metabolites in the biofilms. Therefore, arginine deiminase activity could be important in protection against the acid in biofilm maturation.

1.2.2.3 Pneumococcal surface adhesin A (PsaA)

Pneumococcal surface adhesin A, a metal-binding lipoprotein, is an important virulence factor of the bacterium. The protein is a highly conserved protein that occurred in all 90 serotypes of *S. pneumoniae* (Seo, Seong et al. 2002). The protein displays a crucial role in a pneumococcal adherence to respiratory mucosa (Gor, Ding et al. 2011) and host epithelial cell (Rajam, Anderton et al. 2008). PsaA mutant of *S.*

pneumoniae exhibited the reduction of pneumococcal virulence in a mouse model (Tseng, McEwan et al. 2002).

1.2.2.4 Pneumococcal surface protein A (PspA)

Pneumococcal surface protein A (PspA) is one of an important virulence factors associated with pneumococcal infections. The surface protein is highly immunogenic and common in all serotypes of *S. pneumoniae* (Mayoral, Della et al. 2010). PspA displays a specific receptor for human lactoferrin. The protein interferes complement activation by blocking recruitment of the alternative pathway (Baril, Dietemann et al. 2006). The surface protein is one of effective pneumococcal antigens which confer protection in animal models of streptococcal infections (Oliveira, Miyaji et al. 2010). The protein was found to be good alternative antigen for the conjugated vaccines (Oliveira, Miyaji et al. 2010). PspA mutant of *S. pneumoniae* showed the reduction of pneumococcal infection in a chinchilla Otitis Media model (Schachern, Tsuprun et al. 2014).

1.2.2.5 Pneumococcal surface protein C (PspC)

Pneumococcal surface protein C (PspC), also known as choline-binding protein A (CbpA), is an important virulence factor found in all pneumococci. The molecular structures of PspA and PspC comprise similar structural domains, consisting of a coiled-coil α -helix, followed by a proline-rich region and a choline-binding domain. The α -helical parts of PspA and PspC are unlike, the proline-rich region and choline-binding domains are indigestible (Brooks-Walter, Briles et al. 1999). PspC is a multifunctional virulence factor during *S. pneumoniae* infection. The protein acts as an adhesin protein which bind to a polymeric immunoglobulin receptor including secretory Ig A (Zhang, Mostov et al. 2000). Moreover, PspC interferes the complement system via its capability to bind a complement regulatory protein factor H and a C3 component (Quin, Onwubiko et al. 2007). In addition, the protein is a crucial candidate for a cost-effective vaccine with broad coverage against *S. pneumoniae* diseases (Moreno, Oliveira et al. 2012). Extinction of the surface protein increased the susceptibility to kill by microglia (Peppoloni, Colombari et al. 2006).

1.2.2.6 Pneumolysin

Pneumolysin is a cytoplasmic toxin which acts as a cholesterol-dependent cytotoxin by binding to cholesterol of host cell membrane. The toxin is produced by all clinical isolates of *S. pneumoniae*. Pneumolysin is released by autolytic cells during stationary phase of the bacterial growth (Martner, Dahlgren et al. 2008). The mechanism of action of pneumolysin is thought to follow two stages. Binding of the monomeric toxin to the target cell membrane is occurred in the first stage. The next stage is lateral movement and oligomerisation of the monomers resulting in a large pore formation. The results of the reaction are leakage of intracellular components and influx of water into the cell leading to lysis of the cell (Gillespie and Balakrishnan 2000). Pneumolysin produced by *S. pneumoniae* induced DNA damage and cell cycle arrest in A549 human alveolar epithelial cells (Rai, He et al. 2016). Pneumococcal pneumolysin disrupted autophagosomes leading to escape of *S.pneumoniae* into cytosol (Surve, Bhutda et al. 2018). Pneumococcal infection through pneumolysin release induced progression of established lung fibrosis (Knippenberg, Ueberberg et al. 2015). In addition, the toxin prevented classical pathway of complement by reducing of C3 deposition on the bacterial cells (Yuste, Botto et al. 2005).

1.2.2.7 Autolysin

Autolysin or N-acytyl muramoyl-L-alanine amidase is a major enzyme responsible for cellular autolysis during the end of log phase in *S. pneumoniae*. Autolysin (LytA) causes bacterial lysis by cleaving at lactyl-amide bond of peptidoglycan. The bond is linked with stem peptides and glycan strands of the peptidoglycan. The cleave of the enzyme resulted in hydrolysis of the cell wall (Mellroth, Daniels et al. 2012). Expression of autolysin led to release of pneumolysin and other bacterial components. The release of these factors directly damages host cells and tissues. The enzyme is responsible in autolysis of the cell wall in the response to treatment with antimicrobial agents including deoxycholate or β -lactam antibiotics (Mellroth, Daniels et al. 2012). LytA mutant of *S. pneumoniae* showed the defect of pneumococcal infection in rat meningitis model (Hirst, Gosai et al. 2008).

1.2.2.8 *Streptococcus pneumoniae* hyaluronate lyase (SpnHL)

S. pneumoniae generates various virulence factors to penetrate the physical defenses of the host tissues, including pneumolysin, pneumococcal surface protein A, and hyaluronate lyase (SpnHL). The enzyme is presented on the cell surface of *S. pneumoniae*. SpnHL catalyzes the degradation of hyaluronan, chondroitin, and chondroitin sulfates which are an important constituent of the extracellular matrix of connective tissues (Akhtar and Bhakuni 2003). SpnHL is one of the strategy of the pathogen to obtains carbohydrates for growth during airway colonization (Marion, Stewart et al. 2012). This enzyme is either cell-associated or released outside of cell. SpnHL may be released by the organism to the surrounding host tissues during infection to facilitate bacterial invasion (Akhtar and Bhakuni 2004)

1.2.2.9 Pneumococcal pili

Pili are hair-like appendages found on the surface of many bacteria including *S. pneumoniae*. Initial pneumococcal adhesion and subsequent ability to cause invasive disease is enhanced by pili encoded by *rlr* islet or pilus islet 1 (PI-1) (Barocchi, Ries et al. 2006). Pilus-1 expression is preferentially enhanced at the very early stages of colonization (Pancotto, De Angelis et al. 2013). The expression promotes bacterial penetration through blood-brain barrier in meningitis mouse model (Iovino, Hammarlöf et al. 2016). The pili activate host proinflammatory cytokine including Tumor necrosis factor, and Interlukin-6 during systemic infection (Barocchi, Ries et al. 2006).

1.2.3 Treatment of *S. pneumoniae* infection and incident of antibiotic resistant *S. pneumoniae*

Pneumococcus is a major cause of several human diseases including community-acquired pneumonia, meningitis, septicemia, sinusitis, and otitis media. Pneumonia possesses a crucial health risk to various populations including infants, older adults, workers in hospital, and immunocompromised patients. Community-acquired pneumonia caused by the pathogen is a severe cause of morbidity and mortality worldwide (Zivich, Grabenstein et al. 2018). Treatment for the pneumococcal infection depends on the intensity of the bacterial infection and the general health of

the patient. However, stratagems for treatment, as described in various guidelines, remain argumentative and hard to standardize for all individual and geographic conditions (Niederman, Mandell et al. 2001, Lee, Oh et al. 2018). One of a crucial reason for improvement of the strategy of obvious therapy is related to the variation in the susceptibility patterns of the bacteria. Beta-lactam antibiotic is antibacterial drug of choice for the treatment of *S. pneumoniae* infections (van der Poll and Opal 2009). However, clinical isolates of antibiotic resistant *S. pneumoniae* has been reported (Korona-Glowniak, Zychowski et al. 2018). The organism resists to beta-lactam antibiotics by modification of penicillin-binding proteins.

Macrolide antibiotic including azithromycin, clarithromycin, and erythromycin are used to treat respiratory infections caused by *S. pneumoniae*. However, macrolide resistant pneumococcal isolates have been reported worldwide (Korona-Glowniak, Zychowski et al. 2018). Macrolide resistance in pneumococci is primarily due to two mechanisms including target site modification and efflux pump expulsion (Taha, Araj et al. 2012). The target site modification is involved by *ermB* gene. The presence of the gene leads to reduction in the binding affinity of the antibiotics to the target site. This gene encodes methylase enzyme which relies on methylation of specific adenine residues in 23S rRNA (Taha, Araj et al. 2012). In addition, the presence of methylase enzyme confers to cross resistance to macrolides, sulfamethoxazole-trimethoprim, and tetracycline (Taha, Araj et al. 2012). Macrolide efflux pump is encoded by *mefA/E* genes that confer resistance to several members of macrolide (Sato, Tateda et al. 2011).

Fluoroquinolones such as ciprofloxacin, trovafloxacin, moxifloxacin are used as alternative antibiotics for treatment of lower respiratory tract infections, cause by pneumococci (Patel, McGeer et al. 2011). The target site of fluoroquinolones is DNA gyrase, which catalyzes DNA supercoiling during DNA replication. Fluoroquinolones have potency for the treatment of pneumococcal infection. However, fluoroquinolone resistant strains are mediated by target site modifications which involve DNA gyrase gene mutation (Patel, McGeer et al. 2011). Furthermore, fluoroquinolone resistant pneumococci are mediated by efflux pump system which reduces antibiotic accumulation in the bacterial cells (Jumbe, Louie et al. 2006). In

addition, antimicrobial resistance of *S. pneumoniae* to other antibiotics is increasing worldwide (Table 1)

Table 1. Mechanism of antibiotic resistance in *S. pneumoniae* (Charpentier and Tuomanen 2000)

Antibiotics family	Antibiotic agent	Target	Resistant mechanism
B-lactams	Penicillin	PBP	altered target
	Cephalosporin	PBP	altered target
Fluoroquinolones	Ciprofloxacin	DNA gyrase and topoisomerase IV	altered target, efflux pump
	Sparfloxacin	DNA gyrase and topoisomerase IV	altered target, efflux pump
Macrolides	Erythromycin	23S ribosomal subunit	altered target, efflux pump
Chloramphenicol	Chloramphenicol	50S ribosomal subunit	enzymatic modification
Tetracyclin	Tetracyclin	30S ribosomal subunit	altered target
Diaminopyrimidine	Trimethoprim	DHFR	altered target
Sulphonamide	Sulfamethoxazole	DHPS	altered target

PBP, penicillin binding protein; DHFR, dihydrofolate reductase; DHPS, dihydropteroate reductase.

1.2.4 Diagnosis

Diagnostic methods for pneumonia cause by *S. pneumoniae* have not changed since Pasteur and Sternberg first isolated *S pneumoniae* in 1881, and Christian Gram used his famous stain to disclose the bacterium in 1886 (van der Poll and Opal 2009). The diagnosis of the pneumonia is performed by examining the sputum of patients. The specimen is smeared and stained by Gram stain method. The pathogen is Gram-positive diplococci. The bacteria are cultured on blood agar plate 37° C in 5% CO₂ atmosphere. Pneumococci typically possess α -haemolysis with green discoloration of agar around the colonies on blood agar. Cultures of the bacteria from the specimens including sputum, blood, and other tissue sites should be obtained before obvious antibiotic therapy is started (Mandell, Wunderink et al. 2007). Other methods for diagnosis of pneumococcal infection are now available and can be quite useful. Urinary antigen detection of the polysaccharide from the pneumococcal cell wall by an immunochromatography assay is performed. This assay compares favorably with culture and Gram stain for detection of invasive pneumococcal disease. The method is highly sensitive in severe case of pneumonia and septicemia (Boulware, Daley et al. 2007). The alternative method for pneumococcal diagnosis is non-culture technique based on nucleic acid for *S. pneumoniae*. The method is rapid and highly specific, with pneumococcal-specific DNA sequences as targets for detection process (Abdeldaim, Strålin et al. 2008).

Pneumococcal capsule staining is demonstrated by suspending the bacteria in India ink. In addition, the polysaccharide capsule is typed by the reaction of type specific antibody. The assay is called quellung reaction. The word “quellung” is German for ‘swelling’. The assay is a biochemical reaction in which type specific antibody bind to the pneumococcal polysaccharide capsule. The results of the reaction are precipitation of the large, complex molecule formed, the capsule appears to swell, because of increased surface tension, and its outlines become clearly demarcated. The clearing is best visualized by using a stain to enhance contrast between the clear zone of bound antibody and the surrounding material. *S. pneumoniae* is typically surrounded by one of at least 97 known varieties of polysaccharide capsule, a layer containing chains of monosaccharide which surrounds the cells (Geno, Gilbert et al. 2015).

1.2.5 *Rhodomyrtus tomentosa* (Aiton) Hassk.

1.2.5.1 Botanical description

Rhodomyrtus tomentosa, a flowering plant belongs to the family Myrtaceae, is an evergreen shrub or small tree, up to 4 m tall with dense, short, soft hairs on young stems. *Rhodomyrtus tomentosa* leaves are simple, opposite, entire, oval, obtuse to sharp pointed at the tip, 4.5-8 cm × 2.3-5 cm, glossy green above, densely grey or rarely yellowish-hairy beneath. Flowers are solitary or in group of two or three, 2-3 cm diameter, with 5 petals which are purplish-pink (Figure 1). Fruits are edible, dark purple, round, three or four-celled with many seed. The common names of the plant species are Downy rose myrtle, Downy myrtle, Hill gooseberry, Hill guava, and Isenberg bush.

1.2.5.2 Habitat description

Rhodomyrtus tomentosa is a native to South-East Asia. The plant species is occurred in South-East Asia, India, and Southern China. However, the medicinal plant has been reported as an invasive species in some areas such as Florida, Hawaii. *Rhodomyrtus tomentosa* tolerates full sun and flooding. In Thailand, *Rhodomyrtus tomentosa* has been found in coastal sandy soils on coasts of the Southern and Eastern Thailand.

1.2.5.3 Traditional uses

Rhodomyrtus tomentosa has significant value in traditional medicine for along times. In Malaysia, the fruits of the plant species are used to treat dysentery and diarrhea. Furthermore, diarrhea and stomachache are treated by a decoction of its root and leaf. The decoction is also used as a prospective medicine after birth. *Rhodomyrtus tomentosa* has been used in Indonesian traditional medicine for treatment of wounds. In Vietnam, it has been treated diarrhea and wounds.

1.2.5.4 Chemical components

Rhodomyrtus tomentosa has been reported to contain various phytochemical compositions including triterpenoids (Wai-Haan and Man-Moon 1976), tannins (Liu, Hou et al. 1998), phenolic compounds (Lai, Herent et al. 2013), and

acylphloroglucinols (Salni, Sargent et al. 2002) (Hiranrat and Mahabusarakam 2008). Pure compounds including rhodomentones A and B (Liu, Chen et al. 2016), tomentosenol A, 4S-focifolidione, 4R-focifolidione (Liu, Zhang et al. 2016), tomentodione E (Liu, Song et al. 2018), rhodomyrtals A and B, tomentodiones A-D (Zhang, Chen et al. 2016), members of terpenoids, are isolated from *Rhodomyrtus tomentosa* leaves. Rhodomyrtone, a member of acylphloroglucinols, is originally isolated from the leaves of the plant species (Salni, Sargent et al. 2002).

1.2.5.6 Antibacterial activity and pharmacological effects

Rhodomyrtus tomentosa leaf has been traditionally used to treat many infections. An ethanol extract from *Rhodomyrtus tomentosa* leaf possessed antibacterial activity against a numbers of Gram-positive bacteria including *Bacillus cereus*, *Enterococcus faecalis*, *Listeria monocytogenes*, *Staphylococcus aureus*, *Streptococcus mutans* and *S. pyogenes* (Limsuwan, Trip et al. 2009). Interestingly, the ethanol extract of the plant species exhibited pronounced antibacterial activity against *S. pneumoniae* capsule positive strain (Limsuwan, Trip et al. 2009). The extract possessed anti-staphylococcal activity and anti-biofilm activity against *S. aureus* and *S. epidermidis* (Saising, Ongsakul et al. 2011). Furthermore, the extract reduced established biofilm in both the microorganisms (Saising, Ongsakul et al. 2011). In addition, *S. pyogenes* biofilm was inhibited by the extract via quorum sensing inhibition (Limsuwan and Voravuthikunchai 2008). It has been reported that *S. aureus* treated with the extract showed a reduction in their adhesion to human buccal cells (Limsuwan, Homlaead et al. 2014) and invasiveness in bovine udder epidermal tissue (Mordmuang, Shankar et al. 2015). The extract was significantly effective for the bio-control of *L. monocytogenes* contaminations in cooked chicken meat model (Odedina, Vongkamjan et al. 2016).



Figure 1. *Rhodomyrtus tomentosa* (Aiton) Hassk.

1.2.6 Rhodomyrton

1.2.6.1 Characteristic

Rhodomyrton, a member of acylphloroglucinols, is originally isolated from the leaves of the plant species (Salni, Sargent et al. 2002). Acylphloroglucinols are derivatives of benzene-1,3,5-triol (phlor-oglucinol). Rhodomyrton has been reported to be a small molecule. The molecular weight of the pure compound is 442.6 g/mole (Hiranrat and Mahabusarakam 2008).

1.2.6.2 Antibacterial activity and pharmacological effects

Rhodomyrton demonstrated strong antibacterial activity against wide range of Gram-positive pathogens including methicillin-resistant *S. aureus* (Sianglum, Srimanote et al. 2011), *S. epidermidis* (Saising, Ongsakul et al. 2011), *B. cereus* (Voravuthikunchai, Dolah et al. 2010), and *S. pneumoniae* capsule-producing strains (Limsuwan, Trip et al. 2009). Rhodomyrton inhibited biofilm formation and reduced established biofilm in both *S. aureus* and *S. epidermidis* (Saising, Ongsakul et al. 2011). It has been reported that *S. aureus* treated with rhodomyrton showed a reduction in their adhesion to human buccal cells (Limsuwan, Homlaead et al. 2014) and invasiveness in bovine udder epidermal tissue (Mordmuang, Shankar et al. 2015). In psoriasis experiment, rhodomyrton significantly delayed closure of a wound as revealed by scratch assay. In addition, HaCaT keratinocytes treated with rhodomyrton showed chromatin condensation and fragmentation of nuclei. Moreover, the pure compound induced apoptosis in the keratinocytes (Chorachoo, Saeloh et al. 2016).

1.2.6.3 Antibacterial mode of action

Structural modification of rhodomyrton was monitored to study structure-activity relationship of the compound against pathogenic bacteria. It has been reported that rhodomyrton demonstrated higher antibacterial activity against the tested bacteria than its analogues. The information revealed that hydroxyl and ketone groups of rhodomyrton were illustrated to be essential for the antibacterial property (Leejae, Yingyongnarongkul et al. 2012). Furthermore, rhodomyrton was found in the fraction of cytoplasm of rhodomyrton-treated *S. aureus* (Leejae, Taylor et al. 2013). Thereby,

the major mode of action of the effective compound on the pathogenic bacteria is likely to be inside the cell.

The effects of rhodomyrtone at molecular level have been studied in a few Gram-positive species. Proteomic analysis has revealed that rhodomyrtone affected the expression of several major classes of cellular proteins in methicillin-resistant *S. aureus* (MRSA) (Sianglum, Srimanote et al. 2011). In addition, transcriptome analysis has revealed that rhodomyrtone caused a significant modulation of gene expression, with induction of 64 genes and repression of 35 genes in MRSA (Sianglum, Srimanote et al. 2012). Also, proteomic analysis of rhodomyrtone-treated *S. pyogenes* has shown that the compound affects the expression of streptococcal secreted and whole cell proteins. Most of the altered proteins were identified as enzymes associated with important pathways of the primary metabolism (Limsuwan, Hesselting-Meinders et al. 2011). It has been reported that rhodomyrtone caused large membrane invaginations with an increase in fluidity. It has been documented that rhodomyrtone transiently binds to phospholipid head groups and causes distortion of lipid packing, providing explanations for membrane fluidization and induction of membrane curvature as revealed by molecular dynamics simulation analysis. It has been reported that both its transient binding mode and its ability to form protein-trapping membrane vesicles are unique, making it an attractive new antibiotic candidate with a novel mechanism of action (Saeloh, Tipmanee et al. 2018).

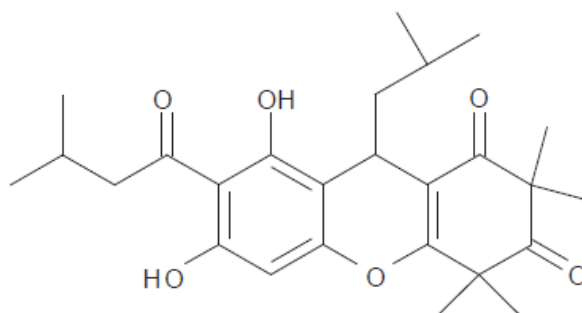


Figure 2. Structure of rhodomyrtone (Limsuwan et al. 2009)

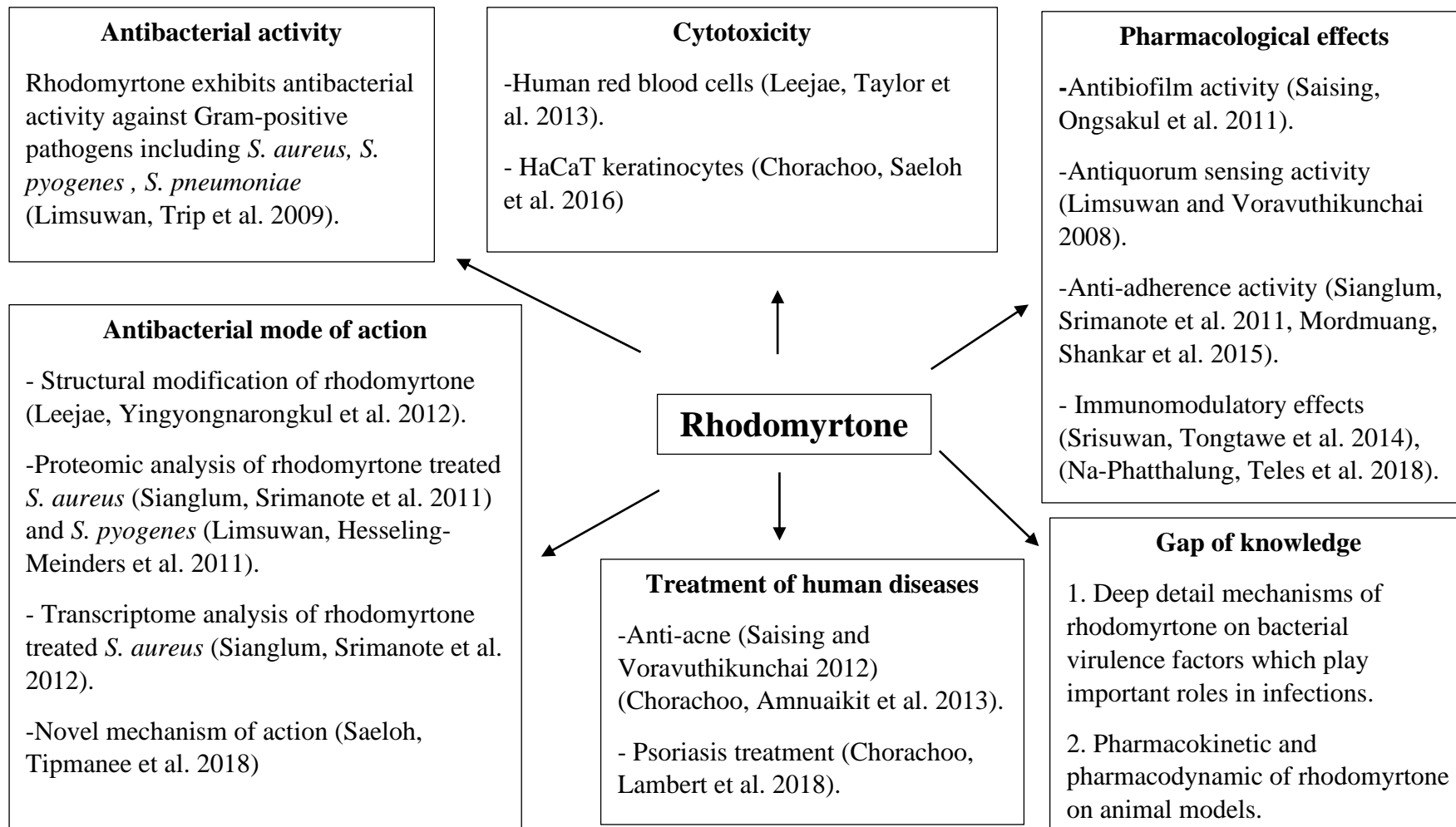


Figure 3. Research representation of rhodomyrton study

1.3 Research objectives

1.3.1 To investigate antibacterial activity of ethanol extract from *Rhodomyrtus tomentosa* leaves, purified rhodomyrtone, and synthetic rhodomyrtone against clinical isolates of *Streptococcus pneumoniae*.

1.3.2 To determine effects of rhodomyrtone on *S. pneumoniae* at molecular levels using proteomic and metabolomic analysis.

1.3.3 To investigate the effects of rhodomyrtone on pneumococcal capsule formation.

1.3.4 To determine the effects of the extract and rhodomyrtone on pneumococcal biofilm.

1.3.5 To monitor the activity of the extract and rhodomyrtone on *S. pneumoniae* adhesion and invasion.

Chapter 2

Research Methodology

2.1 Antibacterial agents

Dried leaves of *Rhodomyrtus tomentosa* were extracted with 95% ethanol. The isolation protocol of rhodomyrtone was performed as described by our research group (Limsuwan, Trip et al. 2009). The ethanol extract, purified rhodomyrtone, and synthetic rhodomyrtone (Sigma) were dissolved in 100% dimethyl sulfoxide (DMSO).

2.2 Bacterial strains and growth conditions

Twenty-three clinical isolates of *S. pneumoniae* were obtained from Hospital Universitario Infantil Virgen del Rocío (HUIVR), Sevilla, Spain. *S. pneumoniae* R6, TIGR4, and Hungary 19A-6 were included as reference strains. The isolates were cultured on blood agar plates at 37 °C for 24 h with 5% CO₂. The organisms were further cultured in Todd-Hewitt broth (THB), and stored in THB containing 30% glycerol at -80 °C until use.

2.3 Cell culture

Monocyte derived macrophage cell line RAW 264.7 and adenocarcinomic human alveolar epithelial cell line A549 were cultured in Dulbecco's Modified Eagle Medium (DMEM) and Roswell Park Memorial Institute 1640 Medium (RPMI 1640), respectively. Both the mediums were supplemented with 10% heat-inactivated bovine serum and antibiotics (penicillin-10 U/ml and streptomycin-10 µg/ml). The cells were allowed to form confluent monolayer cells with 48 h incubation at 37°C in humidified air containing 5% CO₂. Trypsinized cells were seeded into 24-wells to form the monolayer cells (1×10^5 cells/well).

2.4 Determination of minimal inhibitory concentration (MIC) and minimal bactericidal concentration (MBC)

The MIC and MBC values of the ethanol extract and the pure compounds against the isolates were determined using broth microdilution method according to Clinical and Laboratory Standards Institute guidelines (CLSI 2009). The bacteria were inoculated in Mueller-Hinton broth (MHB) supplemented with 2.5% lysed horse blood, and incubated at 37 °C for 6-8 h with 5% CO₂. One hundred microlitre of the bacterial suspension (10⁶ colony forming units/ml, CFU/ml) was added in a 96 well microtiter plate, containing 80 µl of the medium and 20 µl of serially diluted compound, incubated at 37 °C for 18 h with 5% CO₂. The MIC was expressed as the lowest concentration of the extract/compound that inhibits visible growth after incubation. The MBC was expressed as the lowest concentration of the extract/compound that kills the bacteria.

2.5 Time-kill study

S. pneumoniae 5335-5 was grown in MHB with 2.5% lysed horse blood, supplemented with ethanol extract/compound at concentrations of 1/2 ×, 1 ×, 2 ×, and 4 × MIC, and incubated at 37 °C with 5% CO₂. The tested medium containing 1% DMSO was included as negative control. Aliquots were removed at different time intervals (0, 2, 4, 8, 10, 12, 18, and 24 h) and serially diluted. Viable bacteria were calculated by plate counts on blood agar, followed by incubation at 37 °C for 24 h with 5% CO₂.

2.6 Preparation of cellular and secreted proteins

S. pneumoniae strains R6 and TIGR4 were cultured in 200 ml of THB supplemented with 1/2 × MIC purified rhodomirtone or 1% DMSO as control, to an OD₆₀₀ = 0.3. The bacterial cultures were centrifuged at 5,000 × g for 10 min to collect culture supernatant (secreted fraction) and cell pellets. Supernatants were filtered using 0.22-µm filters (Millipore), and proteins were precipitated with 10% trichloroacetic acid and placed overnight on ice. The precipitated proteins were further centrifuged at 13,000 × g for 30 min. The protein pellets were washed 3 times with ice-cold absolute ethanol. The protein samples were dried and dissolved in rehydration buffer (7 M urea,

2 M thiourea, 4% CHAPS, 0.5% Triton X-100, 0.005% bromophenol blue, 0.5% Bio-lyte 3-10 Ampholytes), and kept at -80 °C until use. To obtain bacterial cellular proteins, the cell pellets were washed twice with PBS/30% sucrose. The bacterial cells were lysed by adding 100 U mutanolysin, incubated at 37 °C overnight, and resuspended in rehydration buffer. The samples were sonicated (6 cycles of 20-s pulses, 90% amplitude), and centrifuged at $5,000 \times g$ for 10 min to remove cell debris. Protein-containing supernatants were concentrated using Amicon 10-kDa Ultra-15 Centrifugal Filter Devices (Millipore) according to manufacturer's instructions, and stored at -80 °C until use. The proteins were cleaned with the 2D- Clean-up kit (GE Healthcare). Protein amounts were quantified by the Bradford assay (Bradford 1976).

2.7 Two-dimensional gel electrophoresis (2DE)

One hundred microlitre of protein was subjected to isoelectric focusing (IEF) on 11-cm Immobiline DryStrips immobilized pH gradient (IPG) gel strips (4-7 pH linear gradient (GE Healthcare)). The strips were loaded onto a Bio-Rad Protean IEF Cell system, and IEF was performed at 20 °C using the following conditions: 2 h of passive rehydration, 50 V for 10 h followed by a voltage-ramp (250 V for 15 min; 500 V for 30 min; 2,000 V for 1 h; 6,000 V for 2 h); finally, proteins were focused on 20,000 Vh. For the second dimension, the strips were previously equilibrated in 3 ml equilibration solution (50 mM Tris-HCl pH 8.8; 6 M Urea, 30% glycerol, 2% SDS, 0.002% bromophenol blue) containing 20 mg dithiothreitol and 25 mg iodoacetamide for 15 min at room temperature, respectively. The strips were subsequently placed onto a 1 mm thick 12% polyacrylamide Criterion™ precast gel (Bio-Rad), and covered with warm molten 0.5% agarose. Gels were run at mA/gel until the tracking dye reached the gel bottom. Then, gels were stained with Coomassie brilliant blue G-colloidal solution (Sigma-Aldrich) according to manufacturer's instructions. Gels were scanned with a GS-800 densitometer (Bio-Rad). Digitized images were analyzed with PD-Quest v8.1.0 (Bio Rad). Consistent spots were considered as those whose presence or absence remained constant in overall replicas (3 biological replicates).

2.8 Protein identification by MALDI-TOF/TOF MS

Protein spots of interest were excised from gels and digested automatically employing an Investigator ProPic and ProGest robotic Workstations (Genomic Solutions). Briefly, gel pieces were destained by two washes at 37 °C for 30 min with 200 mM ammonium bicarbonate in 40% (v/v) ACN. Slices were then washed twice, first with 25 mM ammonium bicarbonate for 5 min and later with 25 mM ammonium bicarbonate in 50% (v/v) ACN for 15 min, dehydrated with 100% ACN and finally dried at room temperature for 10 min. Then, 12.5 ng/μl sequence-grade trypsin (Promega) in 25 mM ammonium bicarbonate was added to the gel pieces. Afterwards, the digestion proceeded at 37 °C overnight. Digestion was stopped by adding 10 μl of 0.5% trifluoroacetic acid (TFA); peptides were desalted using μC-18 ZipTip columns (Millipore) and then eluted directly with matrix solution (α -cyanohydroxycinnamic acid at a concentration of 5 mg/ml in 70% ACN/ 0.1% TFA) onto a MALDI plate using the dry droplet method. The mass spectra were acquired in a 4800 Proteomics Analyzer MALDI-TOF/TOF Mass Spectrometer (Applied Biosystems), in the m/z range from 800 to 4,000, with an accelerating voltage of 20 kV in reflectron mode. Spectra were internally calibrated using peptides from trypsin autolysis ($[M+H^+] = 842.509$, $[M+H^+] = 2211.104$) with an m/z precision of ± 20 ppm. The most abundant peptide ions were subjected to MS/MS analysis. A combined search (MS plus MS/MS) was performed against UniProtKB/TrEMBL database using MASCOT (Matrix Science Ltd., London) with the following parameters: taxonomy restrictions to "*Streptococcus pneumoniae*", one missed cleavage, 0.1 Da mass tolerance in MS and 0.2 Da for MS/MS data, Cys carbamidomethylation as a fixed modification and both Met oxidation and Asn/Gln deamidation as variable modifications. Identifications with a Mascot score >70 (P -value < 0.05) were considered as significant.

2.9 Preparation of metabolite extracts

S. pneumoniae strains R6 and TIGR4 were grown in THB with or without $1/2 \times \text{MIC}$ of purified rhodomirtone, incubated at 37 °C with 5% CO₂ to an OD₆₀₀ = 0.3. The bacterial cells were harvested by centrifugation at 5,000 × g for 7 min at 4 °C followed by two washes with PBS to eliminate residual broth. Subsequently, the pellets were resuspended in PBS/30% sucrose. The bacterial cells were lysed as previously described for preparing cellular proteins. Bacterial metabolites were extracted by adding ice-cold methanol to give a final concentration of 50%. Metabolite-containing supernatants were collected and ultracentrifuged at 100,000 × g for 1.5 h, and stored at -80 °C until use.

2.10 Metabolite identification by LC-MS/MS

An Agilent 1200 Series LC system coupled to an Agilent 6540 UHD Accurate-Mass QTOF hybrid mass spectrometer equipped with dual electrospray (ESI) source (Santa Clara, CA, USA) was used. Chromatographic separation was performed using a C18 reverse-phase analytical column (50 mm × 0.46 mm i.d., 3 μm particle size; Teknokroma, Barcelona, Spain), thermostated at 25 °C. The mobile phases were 5% ACN (phase A) and 95% ACN (phase B) both with 0.1% formic acid as ionization agent. The LC pump was programmed with a flow rate of 0.8 ml/min with the following elution gradient: 3% phase B was kept as initial mobile phase constant from min 0 to 1; from 3 to 100% of phase B from min 1 to 13. The injection volume was 3 μl and the injector needle was washed for 10 times between injections with 80% methanol. Furthermore, the needle seat back was flushed for 10 s at a flow rate of 4 ml/min with 80% methanol to avoid cross contamination. The parameters of the electrospray ionization source, operating in negative and positive ionization mode, were as follows: the capillary and fragmentor voltage were set at ±3.5 kV and 175 V, respectively; N₂ in the nebulizer was flowed at 40 psi; the flow rate and temperature of the N₂ as drying gas were 8 l/min and 350 °C, respectively. MS and MS/MS data were collected in both polarities using the centroid mode at a rate of 2.6 spectra per second in the extended dynamic range mode (2GHz). Accurate mass spectra in auto MS/MS mode were acquired in MS *m/z* range 60-1,100 and MS/MS *m/z* range 60-1,100. The instrument

gave typical resolution 15000 FWHM at m/z 118.086255 and 30000 FWHM at m/z 922.009798. To assure the desired mass accuracy of recorded ions, continuous internal calibration was performed during analyses by using the signals at m/z 121.0509 (protonated purine) and m/z 922.0098 [protonated hexakis (1H,1H,3H-tetrafluoropropoxy) phosphazine or HP-921] in positive ion mode; while in negative ion mode ions with m/z 119.0362 (proton abstracted purine) and m/z 966.0007 (formate adduct of HP-921) were used. The auto MS/MS mode was configured with 2 maximum precursors per cycle and an exclusion window of 0.25 min after 2 consecutive selections of the same precursor. The collision energy selected was 20 V. MassHunter Workstation software (version 5.00 Qualitative Analysis, Agilent Technologies, Santa Clara, CA, USA) was used to process all data obtained by LC-QTOF in auto MS/MS mode. The MSMS METLIN Personal Compound and Database Library (PCDL) was used to identify compounds using both MS and MS/MS information to assure metabolite identification.

2.11 Quantification of capsule

Eight encapsulated *S. pneumoniae* isolates representing 8 serotypes (3, 4, 6A, 6B, 14, 18 C, 19 A, and 19 F) were used as representative isolates. The amount of capsule was measured using Stains-all assay (Sigma-Aldrich) for detecting acidic polysaccharides as described (Hammerschmidt et al. 2005), with slight modifications. Briefly, the bacteria were inoculated in THB supplemented with sub-MIC rhodomyrtone and 5% fetal bovine serum to $OD_{600} = 0.5$. Then, 5 ml of the bacterial culture was centrifuged at $5,000 \times g$ for 10 min, washed twice with PBS and resuspended in 600 microlitre of normal saline solution (NSS). One hundred microlitre of the culture was harvested to make dilutions in NSS for plating out to determine the CFU. To quantify acidic polysaccharides, 100 microlitre of the suspension was added in a tube containing 20 mg 1-ethyl-2(3-(1-ethylnaphthho-(1,2-d) thiazolin-2-ylidene) 2 methylpropenyl) naphthho-(1,2-d) thiazolium bromide (Stains-all) and 60 ml glacial acetic acid in 100 ml 50% formamide. The amount of capsule was determined by OD_{640} measuring. One hundred microlitre NSS with 2 ml Stains-all solution was used as a blank.

2.12 Transmission electron microscopy

Pneumococcal capsule was observed using transmission electron microscopy (TEM) as described (Hammerschmidt et al. 2005), but without lysin nor acetate in the cacodylate buffer. Briefly, overnight cultures in THB of *S. pneumoniae* TIGR4 were harvested by centrifugation at $5,000 \times g$ for 10 min. The bacterial cells were washed twice, resuspended in PBS, and fixed with 2% paraformaldehyde and 2.5% glutaraldehyde in 0.1 M cacodylate buffer (pH 7) containing 0.075% ruthenium red for 20 min on ice. The samples were washed with cacodylate buffer containing 0.075% ruthenium red. The samples were fixed again with the fixing solution for 3 h, washed with cacodylate buffer containing 0.075% ruthenium red, and then post-fixed with 1% osmium tetroxide in cacodylate buffer containing 0.075% ruthenium red for 1 h at room temperature. After dehydration in an ascendant series of ethanol, the pieces were transferred to propylene oxide and sequentially infiltrated in EMbed 812 resin (EMS; USA). We used the sequence propylene oxide-resin 2:1, 1:1, and 1:2 throughout 24 h. Afterwards samples were transferred to pure resin for 24 h. Blocks were formed in fresh resin that was allowed to polymerize for 48 h at 65 °C. After trimming, blocks were sectioned in an Ultracut Reicher ultramicrotome to obtain ultrathin (40-60 nm width) sections using a diamond knife. The sections were observed and photographed in a Jeol Jem 1400 Transmission Electron Microscope at the Servicio Centralizado de Apoyo a la Investigacoin (SCAI), University of Cordoba.

2.13 Phagocytosis of *Streptococcus pneumoniae* treated with sub-MICs of the extract and rhodomertone

The bacterial cells were cultured in BHI supplemented with the extract and/or rhodomertone at concentration 1/8, 1/4, and 1/2 \times MIC, or 1% DMSO. The cultures were incubated at 37 °C for 12-16 h with 5% CO₂. The samples were centrifuged at 5,000 g for 5 min, and washed twice by PBS. Monocyte derived macrophage cells were allowed to form confluent monolayer cells with 48 h incubation at 37 °C in humidified air containing 5% CO₂. The trypsinized cells were seeded into 24-wells to form the monolayer cells (1×10^5 cells/well). The monolayer cells were incubated with the bacterial suspensions at cell density of 1×10^6 CFU/well. The bacteria within the macrophages were investigated at different time intervals. The wells

were washed by cold PBS to stop phagocytosis activity. The macrophage cells were then lysed by vigorous pipetting with 0.025 % triton X-100. The numbers of the intracellular pneumococci were serially diluted and counted on blood agar. The plates were incubated at 37 °C for 24 h in humidified air containing 5% CO₂.

2.14 Effects of *Rhodomyrtus tomentosa* ethanol extract and rhodomyrtone on *Streptococcus pneumoniae* biofilm formation

Effects of *Rhodomyrtus tomentosa* ethanol extract and rhodomyrtone on *S. pneumoniae* biofilm formation was assessed by crystal violet assay. Briefly, the bacteria were cultured in MHB supplemented with 2.5% lyzed blood and 1% glucose, incubated at 37 °C for 24 h in 5% CO₂. The overnight culture was diluted to 10⁶ CFU/ml and transferred in a 96-well microtitre plate containing 20 ml tested antibacterial agents at sub-inhibitory concentrations and 80 µl of the medium. The plates were incubated at 37 °C for 24 h in 5% CO₂. The effects of the extract and rhodomyrtone on the growth were measured at OD 600 nm. The wells were washed twice with PBS, air-dried and stained with 200 µl of 0.1% crystal violet solution for 30 min. The wells were washed with water and air-dried. The biofilms were dissolved in 200 µl of 100% DMSO. Inhibitory activity was investigated by quantifying biofilm formation at optical density 570 nm. The relative percentage of biofilm formation was defined as: (mean A570 of treated well/mean A570 of control well) × 100.

2.15 Effects of *Rhodomyrtus tomentosa* ethanol extract and rhodomyrtone on *Streptococcus pneumoniae* established biofilm

Two hundred microlitres of the culture (10⁶ CFU/ml) was transferred to a 96-well microtitre plate and incubated at 37 °C for 2 days (young established biofilm) and 8 days (mature established biofilm). The planktonic cells were removed and replaced with fresh medium every 48 h. After incubation, the medium was removed and the wells were rinsed twice with PBS. The established biofilms were challenged with the agents at concentrations 2-32 × MIC, incubated at 37 °C for 24 h. After incubation, the medium was removed and replaced with 200 µl PBS supplemented with 10 µl 3-(4, 5-dimethylthiazol-2-yl)-2, 5-diphenyltetrazolium bromide, MTT, 5 mg/ml; Sigma) and further incubated at 37 °C for 2 h. The insoluble purple formazan was

obtained by cleavage of MTT by the dehydrogenase enzyme of living bacterial cells. The formazan crystals were dissolved in DMSO and determined by OD 570 measurement. The relative percentage of viability biofilm was defined as: (mean A570 of treated well/mean A570 of control well) \times 100.

2.16 Effects of *Rhodomyrtus tomentosa* extract and rhodomyrtone on pneumococcal adhesion and invasion to A549 human lung adenocarcinoma cell line

The bacterial cells were cultured in BHI medium, incubated at 37 °C for 8 h with 5% CO₂. The cultured bacteria were centrifuged at 5,000 rpm for 5 min, and washed twice. The cells were suspended in PBS, and adjusted to OD 600 = 0.5. The bacterial suspension (5×10^6 CFU/ml) was incubated with the confluent epithelial cells A549 (approximately 1×10^5 cells) and different concentrations of the extract and/or rhodomyrtone at 37 °C in the presence of 5% CO₂. The epithelial cells were washed twice with PBS to remove non-adherent bacteria and lysed with 200 μ l of 0.025% triton X-100. The bacterial cells were counted on blood agar plates. To determine the number of invasive bacteria, the cells were rinsed several times with phosphate-buffered saline (PBS) to remove unbound bacteria. The extracellular bacteria were killed by treatment with gentamicin (100 μ g/ml). The cells were lysed by addition of 0.025% triton X-100 and incubation for 5 minutes at room temperature. The intracellular pneumococci were counted on blood agar plates. The amount of intracellular surviving bacteria per well was determined.

2.17 Statistical analysis

The results are expressed as the mean \pm SE. We performed Student's t-tests to determine statistical differences between control and treatment. *P*-values lower than 0.05 were considered significant difference.

Chapter 3

Results

3.1 *In vitro* antibacterial activity of *Rhodomyrtus tomentosa* ethanol extract and rhodomyrtone against clinical isolates of *S. pneumoniae*

Antibacterial activity of *Rhodomyrtus tomentosa* ethanol leaf extract, purified rhodomyrtone, and synthetic rhodomyrtone against a collection of 23 pediatric *S. pneumoniae* clinical isolates was investigated by broth microdilution assay according to CLSI. As shown in Table 1, minimal inhibitory concentration (MIC) and minimal bactericidal concentration (MBC) values of the ethanol extract ranged from 16-512 µg/ml. Both purified and synthetic rhodomyrtone demonstrated a markedly pronounced antibacterial activity with similar MIC and MBC values ranging from 0.125-4 µg/ml. The MIC and MBC values of the extract, purified rhodomyrtone, and synthetic rhodomyrtone against the reference strains were in the same range as those of the tested clinical isolates. The MIC and MBC values of a positive antibiotic drug, erythromycin, against the clinical isolates is shown in Table 1.

Table 1. Minimal inhibitory concentration (MIC) and minimal bactericidal concentration (MBC) values of *Rhodomyrtus tomentosa* ethanol extract, purified rhodomyrtone, and synthetic rhodomyrtone against *Streptococcus pneumoniae* clinical isolates.

Antibacterial agents	MIC/MBC ($\mu\text{g/ml}$)	
	<i>S. pneumoniae</i> clinical isolates (n=23)	<i>S. pneumoniae</i> ATCC 700673
Ethanol extract	16-256/16-512	32/128
Purified rhodomyrtone	0.125-4/0.125-4	0.50/1
Synthetic rhodomyrtone	0.125-4/0.25-4	1/4
Erythromycin	0.03-2/0.03-4	0.125/0.25

3.2 Time-kill study

To confirm the antimicrobial effectiveness of rhodomyrtone against the pneumococcus, we performed time-kill curves of the three testing preparations at different MICs, using three pneumococcal strains: the reference strains R6 and TIGR4, and the clinical isolate 5335-5, as this presented intermediate MIC/MBC values for rhodomyrtone from the whole collection, but one of the highest MIC/MBC values for erythromycin, a macrolide antibiotic used for treating pneumococcal infections. As shown in Figure 1, 2, and 3, antibacterial activity of the extract and the compounds was concentration dependent, resulting in the reduction of colony forming units. The viability of *S. pneumoniae* after exposure to the extract and the pure compounds at $4 \times$ MIC decreased clearly by 99.9% after 18 h for the three tested strains, and even after 12 h for R6 and TIGR4. Furthermore, addition of the extract and the compounds to the culture at $2 \times$ MIC resulted in decreased cell growth. The extract and the compounds at their MIC values exhibited bacteriostatic effects against *S. pneumoniae* whereas $1/2 \times$ MIC had slight effects on the viability of the tested pathogen.

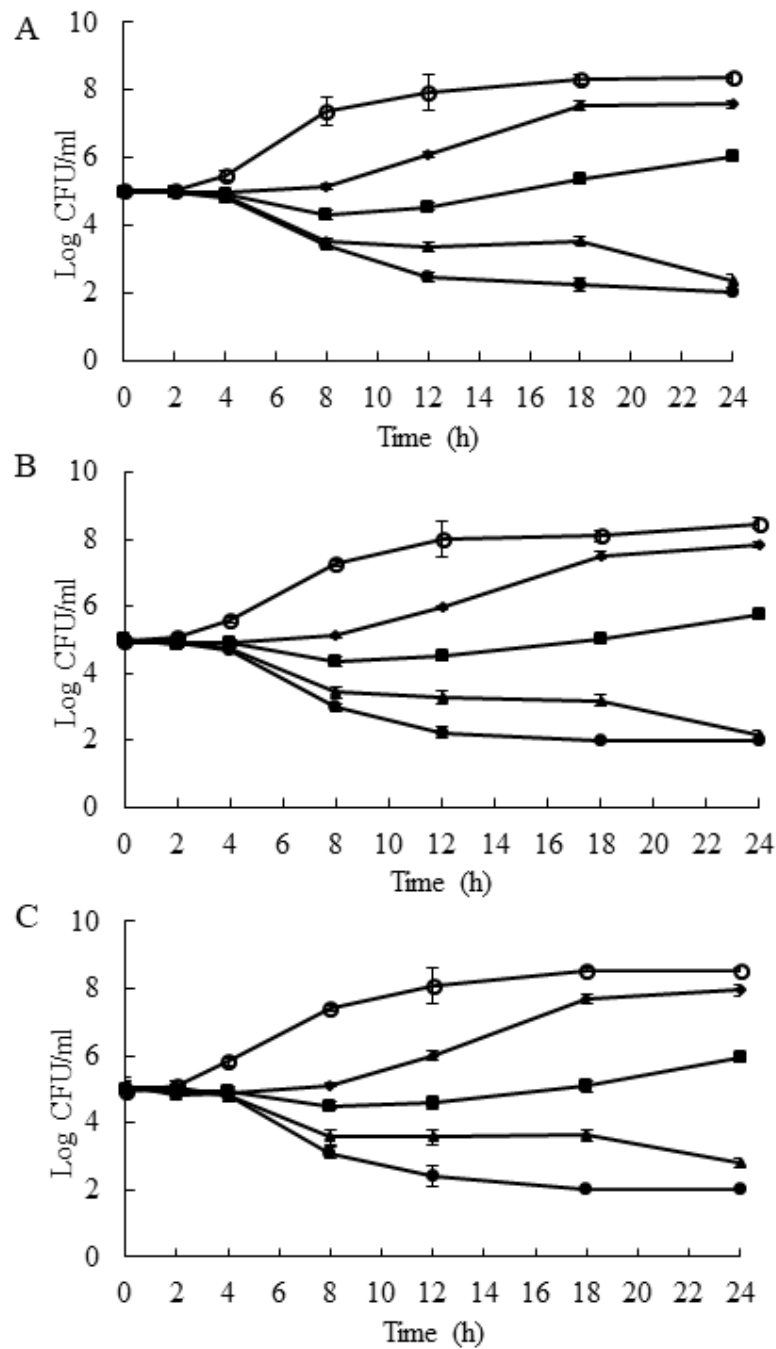


Figure 1. Time-kill curves of *S. pneumoniae* TIGR4 (A), R6 (B) and 5335-5 (C) after treatment with *Rhodomyrtus tomentosa* ethanol extract at 4 × MIC (●), 2 × MIC (▲), 1 × MIC (■), and 1/2 × MIC (◆). One percent of DMSO (○) was used as control. The results are shown as mean ± SD of three independent cultures.

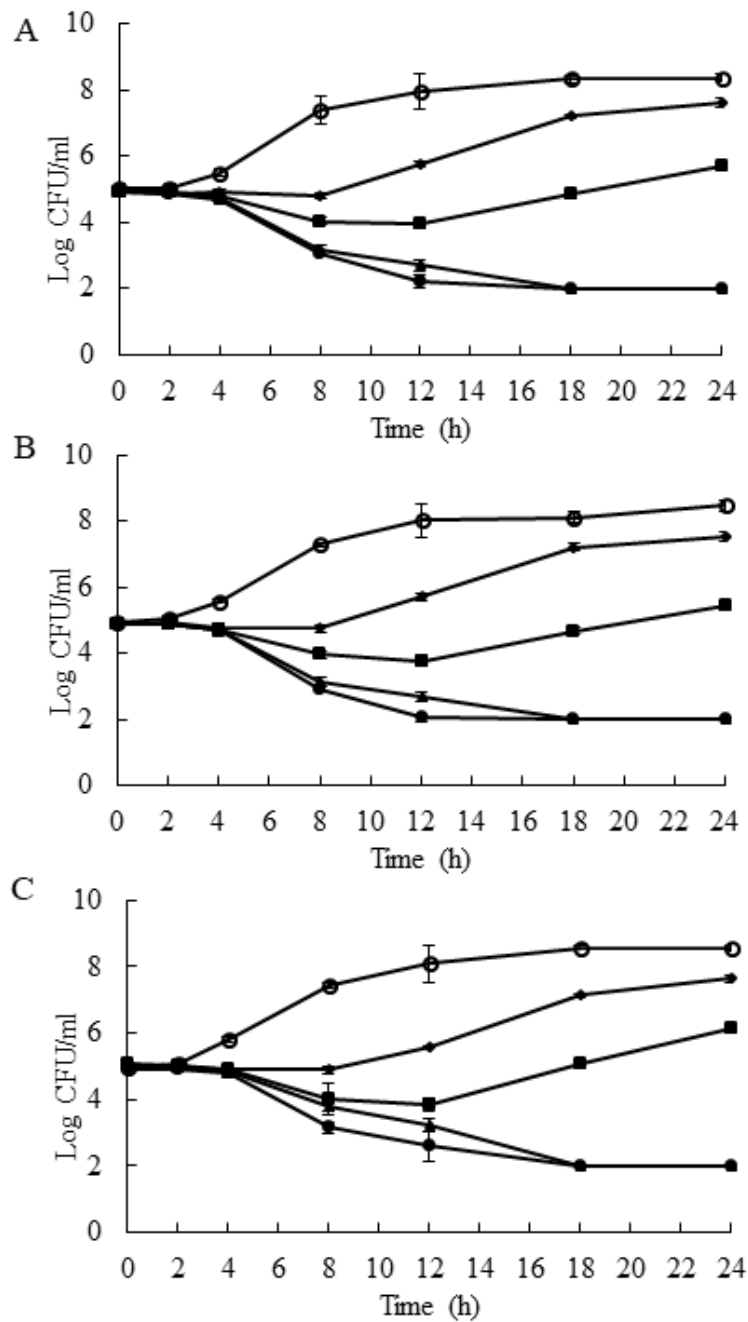


Figure 2. Time-kill curves of *S. pneumoniae* TIGR4 (A), R6 (B) and 5335-5 (C) after treatment with purified rhodomlyrtone at 4 × MIC (●), 2 × MIC (▲), 1 × MIC (■), and 1/2 × MIC (◆). One percent of DMSO (o) was used as control. The results are shown as mean \pm SD of three independent cultures.

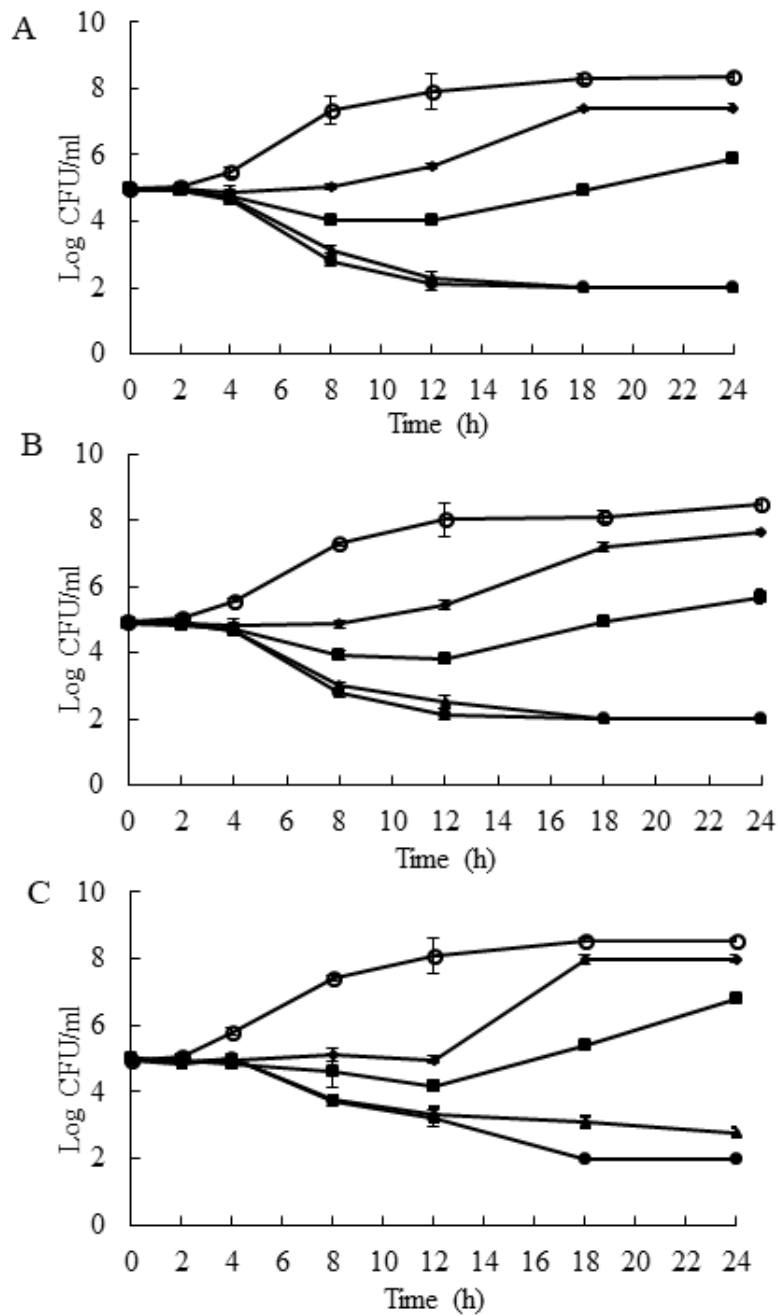


Figure 3. Time-kill curves of *S. pneumoniae* TIGR4 (A), R6 (B) and 5335-5 (C) after treatment with synthetic rhodomyltone at $4 \times \text{MIC}$ (●), $2 \times \text{MIC}$ (▲), $1 \times \text{MIC}$ (■), and $1/2 \times \text{MIC}$ (◆). One percent of DMSO (o) was used as control. The results are shown as mean \pm SD of three independent cultures.

3.3 Effects of purified rhodomyrtone on the pneumococcal growth

In order to investigate the effect of rhodomyrtone at proteomic and metabolomic level, the growth of the reference strains TIGR4 and R6 in the presence of $1/2 \times \text{MIC}$ purified rhodomyrtone was determined. As shown in Figure 2, both strains slowly grew in the antimicrobial-treated cultures. Lag phase of the treated TIGR4 and R6 cells was extended to 8 and 14 h after the bacterial cells started to grow, respectively. The treated TIGR4 and R6 cells reached the stationary phase after 12 and 18 h of incubation, respectively. We chose the mid-log phase for sampling proteins and metabolites, in time points such that for each treated and non-treated culture, the cell growth was the same for both. This corresponded to $\text{OD}_{600} = 0.3$ for TIGR4, and $\text{OD}_{600} = 0.2$ for R6.

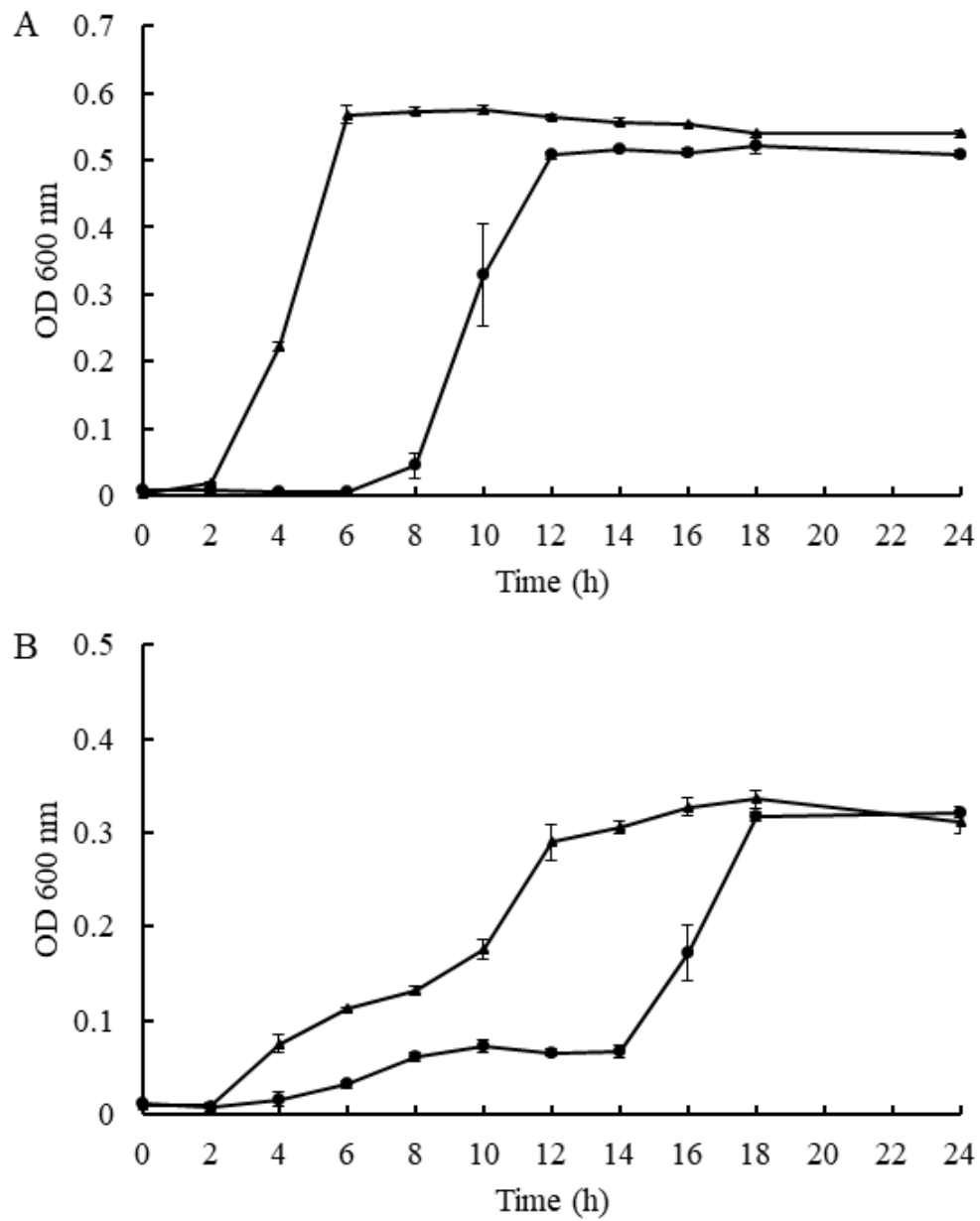


Figure 4. Growth curves of *Streptococcus pneumoniae* strains TIGR4 (A) and R6 (B). The bacteria were treated with $1/2 \times$ MIC rhodomyrtone (▲). One percent DMSO was used as negative control (●).

3. 4 Effects of purified rhodomirtone on the pneumococcal proteome

The changes in the pneumococcal proteome of the two reference strains TIGR4 and R6 after rhodomirtone exposure in two protein fractions, the total cell extract and the secreted proteins were analyzed by 2 DE. The cellular and secreted protein patterns of both strains are shown in Figures 5 and 6, respectively. Alteration in the abundance of 72 protein spots was observed when *S. pneumoniae* was exposed to $1/2 \times \text{MIC}$ purified rhodomirtone. Sixteen cellular protein spots were decreased, while 8 spots were increased in TIGR4 (Figure 5A and 5B). In R6, 20 spots decreased and 7 increased their abundances after rhodomirtone exposure (Figure 5C and 5D). In the secreted fraction, 5 spots of TIGR4 proteins were reduced after rhodomirtone treatment, while 2 spots increased them (Figure 6A and 6B). In the R6 strain, 7 spots increased and other 7 decreased in response to rhodomirtone (Figure 6C and 6D). The selected protein spots were further analyzed by MALDI-TOF/TOF MS. The identified proteins for both cellular and secreted fractions are given in Tables 2 and 3, respectively. The proteins were identified as enzymes involved in important metabolic pathways such as amino acid, carbohydrate, lipid, and nucleic acid metabolism, as well as other factors involved in protein synthesis.

The combined analysis of both cellular and secreted proteomes revealed that proteins related to protein synthesis, as cysteine synthase and ribosomal proteins, decreased in response to purified rhodomirtone treatment, as well as the elongation factor Tu, which was strongly reduced. A clear decrease in two out of the three enzymes of the arginine deiminase (ADI) pathway, i.e. arginine deiminase and ornithine carbamoyltransferase was also found. Furthermore, we observed a down-regulation of proteins involved in carbohydrate metabolism. Important enzymes associated with the glycolysis pathway including glyceraldehyde-3-phosphate dehydrogenase, fructose-1,6-diphosphate aldolase, and triosephosphate isomerase were diminished. However, an increase in the levels of glucose-6-phosphate isomerase, enolase, phosphoglycerate kinase, and 6-phosphofructokinase were observed after rhodomirtone treatment. There was also a decrease in the enzymes L-lactate dehydrogenase and acetate kinase, involved in pyruvate metabolism. A decrease in the levels of 3-oxoacyl-(acyl-carrier-protein) reductase, an enzyme involved in the fatty acid biosynthesis pathway, was also

observed in R6 cellular protein fractions, as well as a decrease in the DNA gyrase A subunit, a target for quinolone antibiotics (Table 2 and 3).

A very interesting finding from the proteomic analysis was the decrease in two enzymes taking part in the synthesis of the pneumococcal capsule polysaccharide: the UTP-glucose-1-phosphate uridylyltransferase (GalU), which diminished in rhodomertone-treated TIGR4 cellular protein fractions, and the family-2 glycosyltransferase encoded in the locus *spr0136*, which diminished after exposure of R6 to the compound. In both cases, the corresponding protein spots were absent in the cellular-protein 2-D gels.

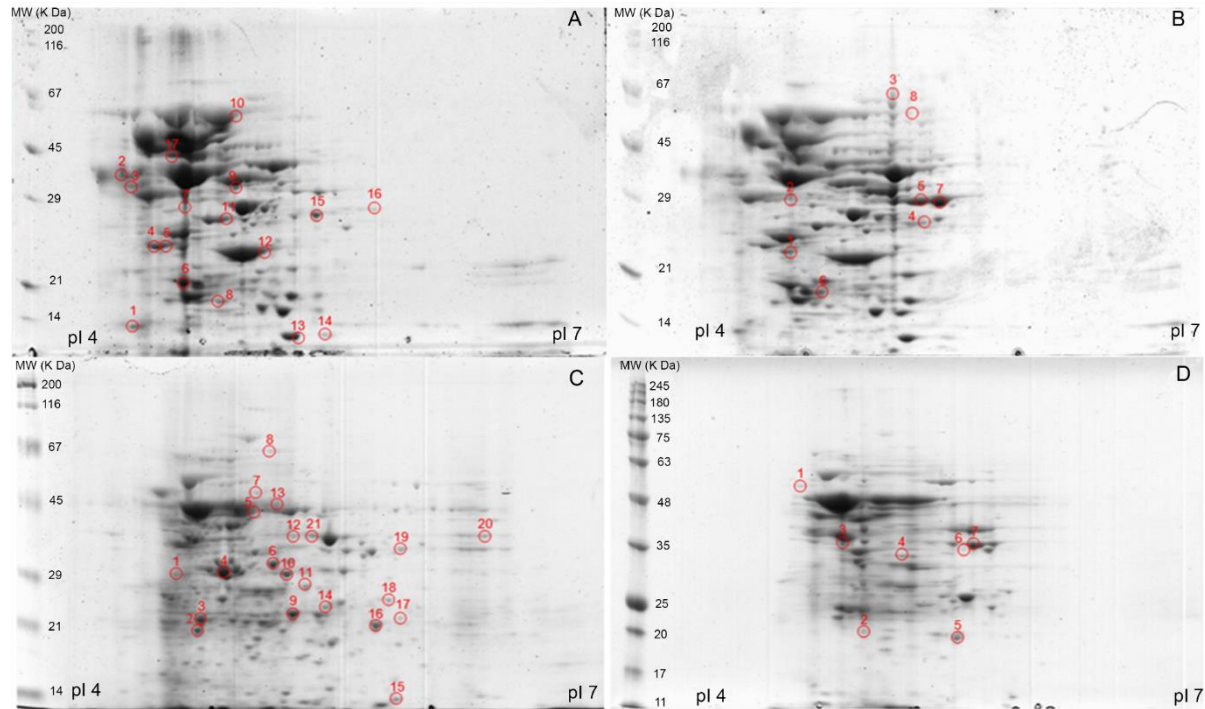


Figure 5. Representative 2-D gels of cellular proteins of *S. pneumoniae* TIGR4 (A and B) and R6 (C and D) cultured without (A and C) and with $1/2 \times$ MIC purified rhodomlyrtone (B and D). The isolated proteins were separated by isoelectric focusing in the pI range of 4 to 7 in the first dimension (11 cm). The proteins were further separated by 10% SDS-PAGE in the second dimension. Spot numbers indicate spots with altered abundances: those marked in A and C diminished after rhodomlyrtone treatment, and those marked in B and D augmented after rhodomlyrtone exposure.

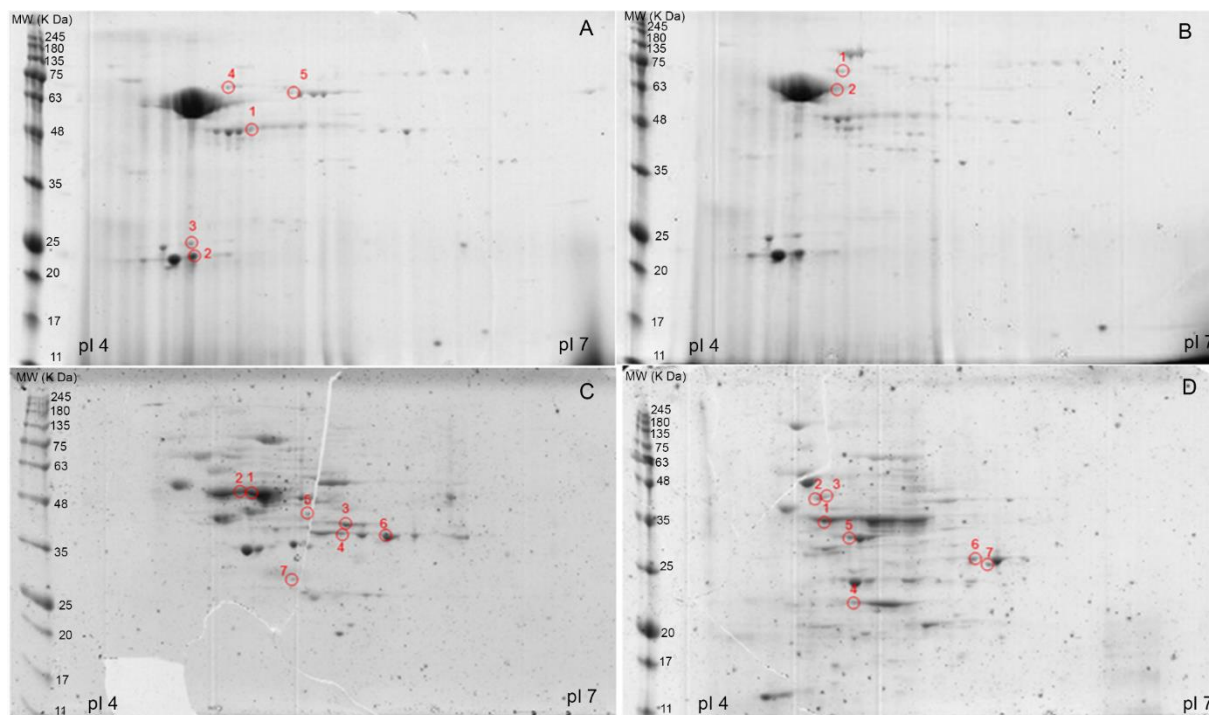


Figure 6. Representative 2-D gels of secreted proteins of *S. pneumoniae* TIGR4 (A and B) and R6 (C and D) cultured without (A and C) and with $1/2 \times$ MIC purified rhodomlyrtone (B and D). The isolated proteins were separated by isoelectric focusing in the pI range of 4 to 7 in the first dimension (11 cm). The proteins were further separated by 10% SDS-PAGE in the second dimension. Spot numbers indicate spots with altered abundances: those marked in A and C diminished after rhodomlyrtone treatment, and those marked in B and D augmented after rhodomlyrtone exposure.

Table 2. Cellular proteins altered after purified rhodomyrone treatment of *Streptococcus pneumoniae*

Spot	Accession number ^a	Protein annotation	Mascot score	Coverage (%)	Fold change ^b	P-value ^c
4C	Q8DMY8	Cysteine synthase	180	21	0.36	0.032
10C	Q8DN31	Arginine deiminase	316	19	0.41	0.018
12C, 21C	P65608	Ornithine carbamoyltransferase	158	23	0.31	0.021
4A	Q97NL1	Glyceraldehyde-3-phosphate dehydrogenase, type I	308	30	0.29	0.019
6A	P66942	Triosephosphate isomerase	104	24	0.33	0.028
11A, 6C, 11C	P0A3M9, P0A3N0	L-lactate dehydrogenase	101	22	0.44	0.045
14A	P58313	UTP-glucose-1-phosphate uridylyltransferase	103	31	0.38	0.010
1C	Q8DRG7	Glycosyltransferase, family 2	98	25	0.30	0.013

Table 2. Cellular proteins altered after purified rhodomyrone treatment of *Streptococcus pneumoniae* (Continued)

Spot	Accession number ^a	Protein annotation	Mascot score	Coverage (%)	Fold change ^b	P-value ^c
16C	Q8DR15	3-ketoacyl-(acyl-carrier-protein) reductase	95	20	0.37	0.023
7C	Q8DPM2	DNA gyrase A subunit	96	21	0.40	0.039
5C	P64031	Elongation factor Tu	517	26	0.29	0.009
6B	Q97SV1	50S ribosomal protein L5	87	18	1.93	0.034
3D	Q8DN74	Glucose-6-phosphate isomerase	83	19	2.41	0.022
7B	P64022	Elongation factor G	348	24	2.75	0.043

^aAccession numbers correspond to UniProt. ^bThe values represent the intensities ratio between rhodomyrone treatment and control for each spot. Values >1 indicate an increase in protein abundance. Values <1 indicate a decrease in protein abundance.

^cData were analyzed using the Student's *t*-test. *P*-values < 0.05 were considered statistically significant.

Table 3. Secreted proteins altered after purified rhodomyrone treatment of *Streptococcus pneumoniae*

Spot	Accession number ^a	Protein annotation	Mascot score	Coverage (%)	Fold change ^b	P-value ^c
3C	P65608	Ornithine carbamoyltransferase	355	25	0.38	0.023
5C	P63414	Acetate kinase	104	23	0.40	0.033
6C	Q8CWN6	Glyceraldehyde-3-phosphate dehydrogenase	403	32	0.037	0.037
2C	P64031	Elongation factor Tu	520	29	0.39	0.029
7C	P0A4S2	Fructose-1,6-bisphosphate aldolase	139	22	0.48	0.047
2D	Q8DPS0	Enolase	396	30	2.54	0.018
5D	Q8DQX8	Phosphoglycerate kinase	848	31	1.97	0.026
7D	Q8DQ85	6-phosphofructokinase	154	26	2.66	0.017
4D	Q8CWV4	50S ribosomal protein L5	81	20	1.85	0.040
3D	Q6VB96	60 kDa chaperonin	230	29	2.11	0.024

^aAccession numbers correspond to UniProt. ^bThe values represent the intensities ratio between rhodomyrone treatment and control for each spot.

Values >1 indicate an increase in protein abundance. Values <1 indicate a decrease in protein abundance.

^cData were analyzed using the Student's *t*-test. *P*-values < 0.05 were considered statistically significant.

3.5 Effects of purified rhodomyrtone on the pneumococcal metabolome

The changes of the metabolomic profile of both strains of *S. pneumoniae* treated with the compound were monitored using LC-MS/MS analysis. We carried out a multivariate statistical analysis with the identified compounds to evaluate whether the rhodomyrtone treatment had a significant effect on the metabolite profile. As shown in Figure 7, a principal component analysis (PCA) resulted in a clear distinction between rhodomyrtone-treated and non-treated metabolite fractions for both R6 and TIGR4 strains. The first principal component (PC1, X-axis) was able to completely separate the two samples, i.e. control and rhodomyrtone-exposed cultures for the two strains, grouping the three biological replicates in the same cluster, each analyzed in duplicate. Thus, the PC1 was able to explain most of the variance that was found. This indicates that the rhodomyrtone treatment lead to a clear alteration of the metabolite profile in the two studied pneumococcal strains.

Alteration in the metabolite expression is shown in Table 4. Twenty-six metabolites were detected to change between both control and treatment groups. Eighteen metabolites were found with lower levels after rhodomyrtone treatment, while nine metabolites were more abundant after treatment with the compound. The most highlighting findings of the metabolomic analysis was the alteration of metabolites involved in capsule biosynthesis, in agreement with the results obtained in the proteomic analysis. Three compounds clearly decreased their levels after rhodomyrtone treatment: two in both strains (uridine 5'-diphosphoglucuronic acid, 1.69-fold and 3.0-fold in R6 and TIGR4 respectively; UDP-glucose, 1.31-fold and 1.27-fold in R6 and TIGR4 respectively), and one in TIGR4 only (UDP-N-acetyl-D-galactosamine, 3.12-fold decrease). In addition, other metabolites involved in the synthesis of nucleic acids and amino acids were also altered, in agreement to the fact that some of the pathways were found altered according to the proteomic analysis. Of note, it is worthy to highlight the almost 2-fold decrease in the levels of acetyl-CoA, a key intermediate in different metabolic pathways playing a central role in the primary metabolism.

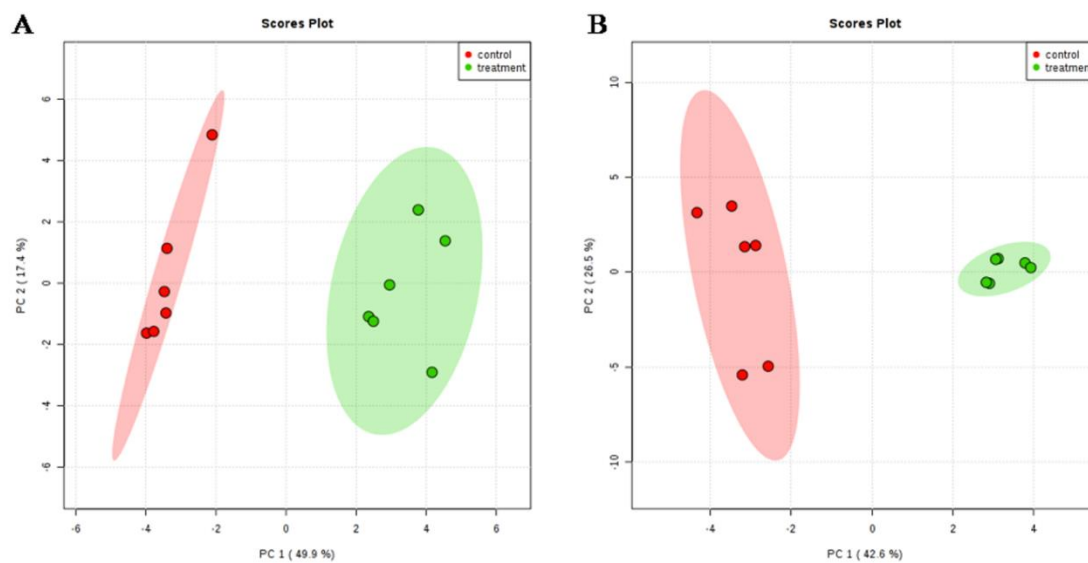


Figure 7. Principal component analysis of the metabolite profile of *Streptococcus pneumoniae* strains TIGR4 (A) and R6 (B) treated with $1/2 \times$ MIC rhodomyrtone.

Table 4. Metabolites altered after rhodomlyrtone treatment of *Streptococcus pneumoniae*

Metabolite	Strain	MW (g/mol)	Retention time (min)	Precursor ion (m/z)	Fold changes ^a	Related pathway
Metabolites with decreased abundance						
Thymidine monophosphate (dTMP)	R6, TIGR4	322.0566	2.7	321.0494	13.49*, 1.71	Nucleic acid biosynthesis
L-Tryptophan	R6, TIGR4	204.0899	4.8	205.0970	1.34*, 1.70*	Amino acid biosynthesis
Uridine 5'-diphosphoglucuronic acid	R6, TIGR4	580.0343	1.1	579.0279	1.69*, 3.00*	Capsule synthesis
N-Acetyl-L-glutamic acid	R6, TIGR4	189.0637	1.8	188.0560	2.11*, 1.09	Urea cycle
UDP-glucose	R6, TIGR4	566.0550	1.1	565.0473	1.31, 1.27*	Capsule synthesis
Hypoxanthine	R6, TIGR4	136.0385	1.6	137.0456	1.02, 2.21*	Nucleic acid biosynthesis

Table 4. Metabolites altered after rhodomyrtone treatment of *Streptococcus pneumoniae* (Continued)

Metabolite	Strain	MW (g/mol)	Retention time (min)	Precursor ion (m/z)	Fold changes ^a	Related pathway
Metabolites with decreased abundance						
Deoxyinosine	R6	252.0859	3.7	251.0771	INF ^b	Nucleic acid biosynthesis
Guanosine	R6, TIGR4	283.0917	2.2	284.0994	1.01, INF	Nucleic acid biosynthesis
Inosine	R6	268.0808	3.3	267.0744	1.07	Nucleic acid biosynthesis
D-(+)-3-Phenyllactic acid	R6, TIGR4	166.0629	6.6	165.0540	INF, INF	Antimicrobial compound
L-Aspartic Acid	TIGR4	133.0375	1.0	132.0297	1.35	Amino acid biosynthesis

Table 4. Metabolites altered after rhodomyrtone treatment of *Streptococcus pneumoniae* (Continued)

Metabolite	Strain	MW (g/mol)	Retention time (min)	Precursor ion (m/z)	Fold changes ^a	Related pathway
Metabolites with decreased abundance						
N-Acetyl-DL-methionine	TIGR4	191.0616	5.1	190.0539	4.77*	Oxidative stress response
Acetyl-CoA	TIGR4	809.12577	5.0	403.5561	1.98*	Lipid metabolism, intermediate molecule
Raffinose	R6	504.169	1.2	503.1623	2.03*	Raffinose/stachyose Melibiose transport system
Deoxy adenosine monophosphate	TIGR4	331.0682	1.6	332.0747	1.04	Nucleic acid biosynthesis

Table 4. Metabolites altered after rhodomyrton treatment of *Streptococcus pneumoniae* (Continued)

Metabolite	Strain	MW (g/mol)	Retention time (min)	Precursor ion (m/z)	Fold changes ^a	Related pathway
Metabolites with decreased abundance						
Palmitic acid	R6, TIGR4	256.2402	0.4	257.2472	1.09, 1.38	Lipid biosynthesis
UDP-N-acetyl-D-galactosamine	TIGR4	607.0816	1.2	606.0742	3.12*	Capsule synthesis
Pyroglutamic acid	R6	129.0426	1.5	128.0354	3.77*	Amino acid metabolism
Metabolites with increased abundance						
Guanosine monophosphate	R6, TIGR4	363.058	1.5	362.0516	3.38*, 2.32*	Nucleic acid biosynthesis
L-Tyrosine	R6	181.0739	1.8	180.0666	1.08	Amino acid biosynthesis

Table 4. Metabolites altered after rhodomyrtone treatment of *Streptococcus pneumoniae* (Continued)

Metabolite	Strain	MW (g/mol)	Retention time (min)	Precursor ion (m/z)	Fold changes ^a	Related pathway
Metabolites with increased abundance						
Uridine monophosphate (UMP)	R6, TIGR4	580.0343	1.1	579.0279	4.73*, 1.37*	Nucleic acid biosynthesis
D-Ribulose 5-phosphate	R6	230.0192	0.7	229.0120	1.05	Pentose phosphate pathway
D-Glucose 6-phosphate	R6, TIGR4	260.0297	0.7	259.0226	1.71, 5.25*	Glycolysis
Cyclic adenosine diphosphate ribose	R6, TIGR4	541.0611	1.4	540.0545	2.85*, 1.04	Calcium signaling
L-Glutamate	R6, TIGR4	147.0532	0.7	146.0456	1.37, 1.44*	Amino acid biosynthesis

Table 4. Metabolites altered after rhodomirtone treatment of *Streptococcus pneumoniae* (Continued)

Metabolite	Strain	MW (g/mol)	Retention time (min)	Precursor ion (m/z)	Fold changes ^a	Related pathway
Metabolites with decreased abundance						
L-Phenylalanine	R6	165.079	3.5	166.0857	1.69*	Amino acid biosynthesis

^aThe fold change values represent the ratio between control and rhodomirtone treatment for metabolites with decreased abundance, or the ratio between the rhodomirtone treatment and the control for metabolites with increased abundance. Statistical significance of the analysis under the Student's *t*-test is indicated as * ($p < 0.05$).

^bINF means that the metabolite was not detected in the rhodomirtone-treated samples.

3.6 Effect of purified rhodomyrtone on the pneumococcal capsule

The results from both proteomic and metabolomic analyses revealed that purified rhodomyrtone reduced the levels of biomolecules involved in the biosynthesis of the pneumococcal capsule. Hence, we studied the effects of the compound on pneumococcal capsule formation.

The inhibitory activity of purified rhodomyrtone on pneumococcal capsule formation was assessed on 8 clinical isolates of *S. pneumoniae* representing 8 serotypes. The amount of pneumococcal capsular polysaccharide produced by the cells treated with sub-MIC rhodomyrtone was quantified by the colorimetric Stains-all assay. The compound caused a reduction of capsule production in a concentration-dependent manner, resulting in a reduction of capsular polysaccharide contents (Figure 8A). However, the tested sub-MICs rhodomyrtone had no inhibitory effects on the growth of *S. pneumoniae* clinical isolates (Figure 8B), thus indicating that the lower amount of measured capsule was not due to a lower number of cells grown in the cultures. Rhodomyrtone-treated pneumococcal cells significantly possessed less amount of capsule, when compared with untreated cells. The reduction in capsular polysaccharide contents was greatest when the bacteria were treated with $1/2 \times$ MIC rhodomyrtone. At this concentration, the percent reduction of capsular polysaccharide formation of *S. pneumoniae* serotypes 3, 4, 6A, 6B, 14, 18C, 19A, and 19F by rhodomyrtone were 75, 80, 33, 62, 43, 53, 67, and 57%, respectively. The highest reduction was observed in serotype 4, with percentages ranging from 29-80%.

We also observed changes, at a qualitative level, in the presence, morphology and/or thickness of pneumococcal capsule in the reference strain TIGR4 treated with the compound using transmission electron microscopy (Figure 9). Rhodomyrtone-treated TIGR4 cells clearly possessed less amount of capsule, when compared with untreated cells (Figures 9C, 9D).

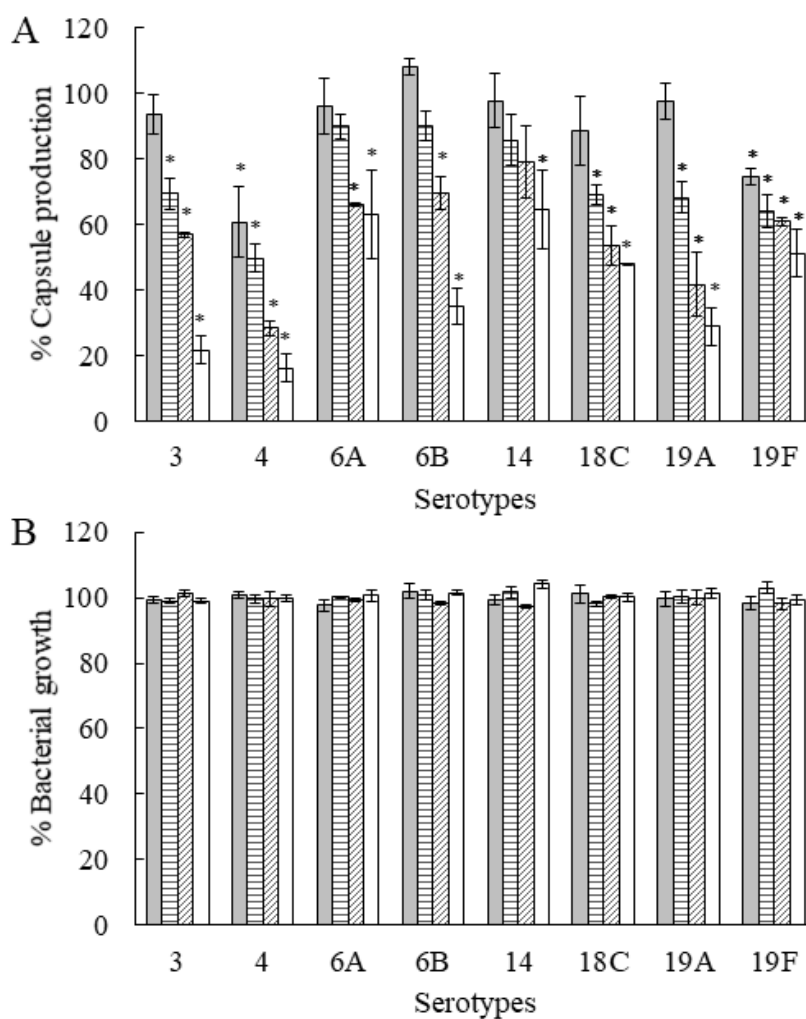


Figure 8. Inhibition of pneumococcal capsule by purified rhodomlyrtone. Effects of purified rhodomlyrtone at different concentrations including $1/16 \times \text{MIC}$ (□), $1/8 \times \text{MIC}$ (▤), $1/4 \times \text{MIC}$ (▨), and $1/2 \times \text{MIC}$ (□) on percentage of pneumococcal capsule (A) and growth (B), compared with control (1% DMSO). The relative percentage of capsule formation was defined as: (mean A640 of treated cells/mean A640 of control) $\times 100$.

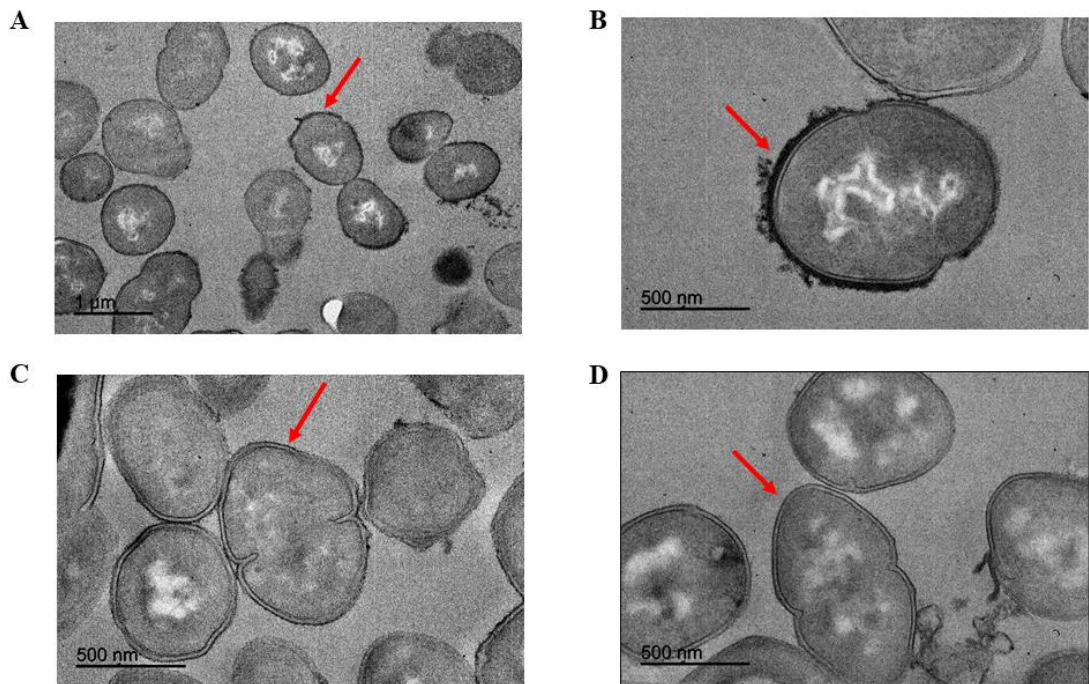


Figure 9. Capsular illustration by transmission electron microscopy of *S. pneumoniae* TIGR4 cells before (A, B) and after exposure to $1/2 \times \text{MIC}$ purified rhodomyrone (C, D). Arrow shows capsule of the bacteria.

3.7 Phagocytosis of *S. pneumoniae* treated with sub-MICs of the extract and rhodomyrtone

Expression of two enzymes (glycosyltransferase and galU) and three metabolites (UDP-Glc, UDP-Glc-UA and UDP-N-acetyl-D-galactosamine) involved in the synthesis of pneumococcal capsule was suppressed upon exposure to rhodomyrtone. It was found that rhodomyrtone-treated pneumococcal cells significantly possessed less amount of capsule when compared with the untreated cells. Capsule polysaccharide of *S. pneumoniae* plays a role against phagocytosis. Hence, inhibition of pneumococcal capsule formation by rhodomyrtone could enhance bacterial phagocytosis by macrophages. The present study investigated phagocytosis of pneumococci treated with the extract and rhodomyrtone using RAW264.7 macrophage cells. Significant increase in phagocytosis of pneumococci was observed when the bacteria were treated with sub-MICs of the extract (Figure 10) and rhodomyrtone (Figure 11) within 10 minutes ($P < 0.05$). Increase in 90-99% phagocytosis of the bacterial cells by the macrophage cells was detected following the treatment with the extract and rhodomyrtone at $1/2 \times \text{MIC}$, compared with the control.

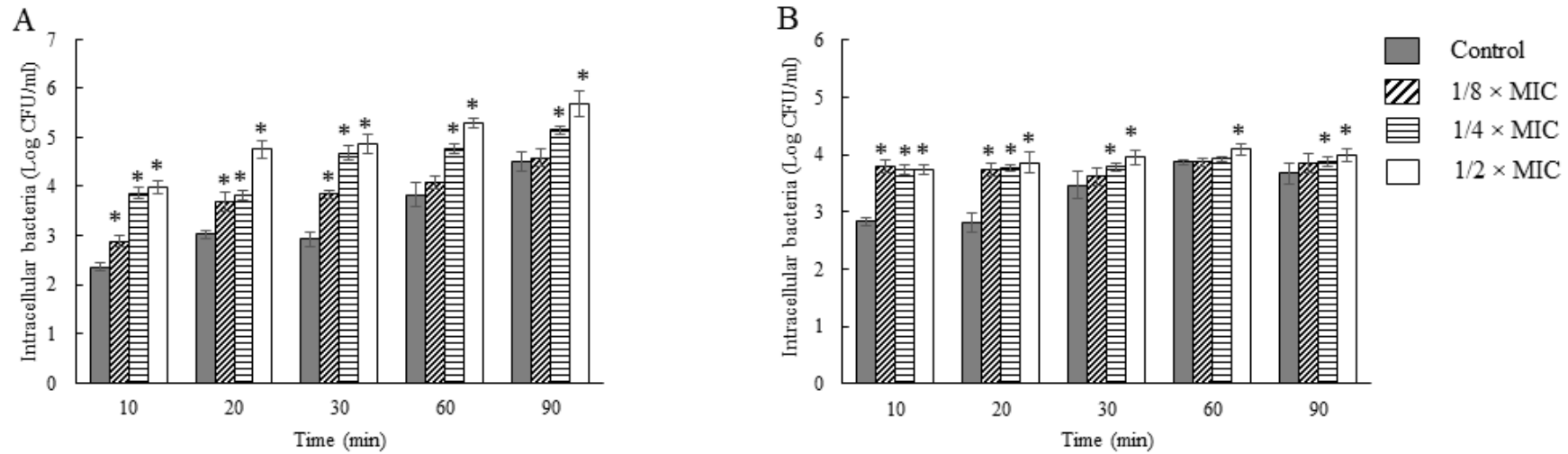


Figure 10. Activity of *Rhodomyrtus tomentosa* ethanol extract on phagocytosis of *S. pneumoniae* NPRCoE 16507 (A) and ATCC 49619 (B). The bacteria were treated with the extract at sub-MICs. The treated cells were further incubated with monocyte-derived macrophage RAW264.1 at 37°C under 5% CO₂. The viable cells of *S. pneumoniae* were counted on blood agar plates, and incubated at 37°C under 5% CO₂. Data are presented as a mean ± SD, (* significant difference; $P < 0.05$).

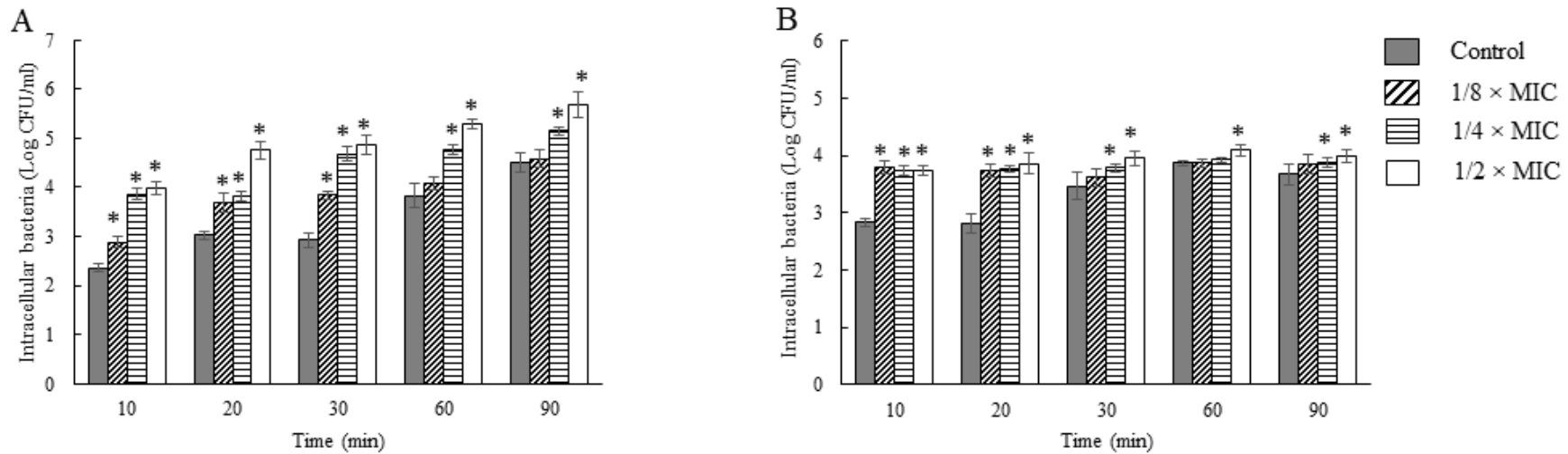


Figure 11. Activity of rhodomirtone on phagocytosis of *S. pneumoniae* NPRCoE 16507 (A) and ATCC 49619 (B). The bacteria were treated with rhodomirtone at sub-MICs. The treated cells were further incubated with monocyte-derived macrophage RAW264.1 at 37°C under 5% CO₂. The viable cells of *S. pneumoniae* were counted on blood agar plates, and incubated at 37°C under 5% CO₂. Data are presented as a mean ± SD, (* significant difference; $P < 0.05$).

3.8 *Rhodomyrtus tomentosa* leaf ethanol extract and rhodomyrtone inhibit biofilm formation in *S. pneumoniae*

The potential of *Rhodomyrtus tomentosa* extract (Figure 12B) and rhodomyrtone (Figure 13D) as inhibitors against *S. pneumoniae* biofilm formation was assessed by crystal violet assay. The extract and rhodomyrtone at $1/8 \times \text{MIC}$ significantly inhibited pneumococcal biofilm formation in all isolates ($P < 0.05$) without growth inhibition. It was observed that growth of the isolates was significantly inhibited by the extract at $1/4$ and $1/2 \times \text{MIC}$ (Figure 12A). This may be due to other compounds present in the extract (Liu, Tan et al. 2016).

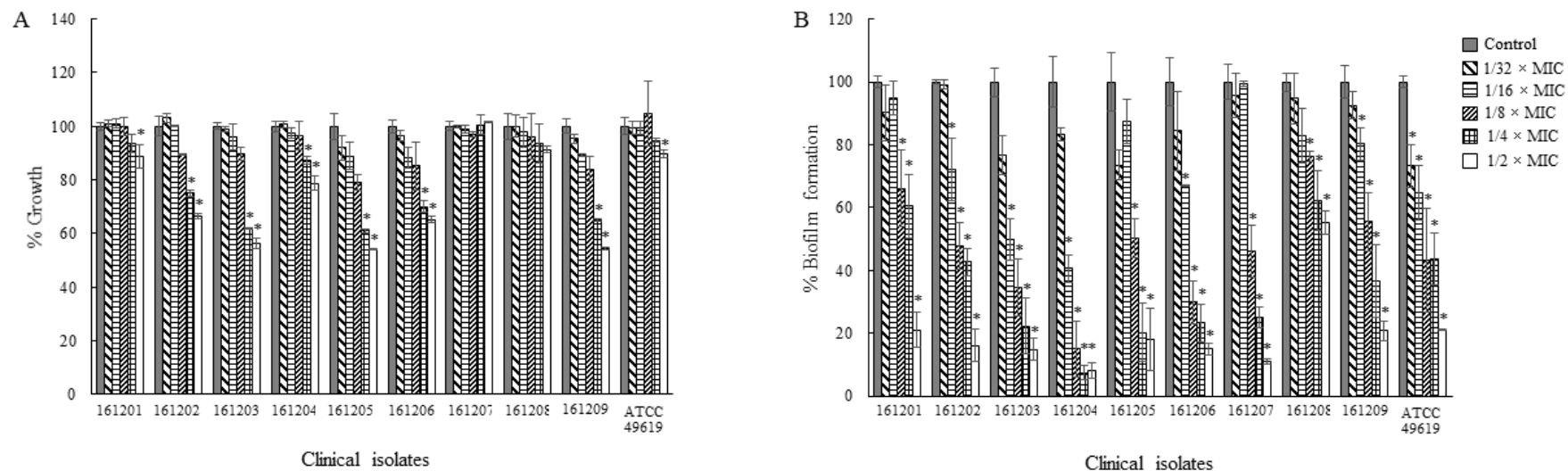


Figure 12. Effects of *Rhodomyrtus tomentosa* ethanol extract on *Streptococcus pneumoniae* growth (A) and biofilm formation (B). The bacteria were cultured in the tested medium supplemented with *Rhodomyrtus tomentosa* extract at sub-MICs. 1% DMSO was used as negative control. The relative percentage of biofilm formation was defined as: (mean A570 of treated well/mean A570 of control well) × 100, (* significant difference; $P < 0.05$).

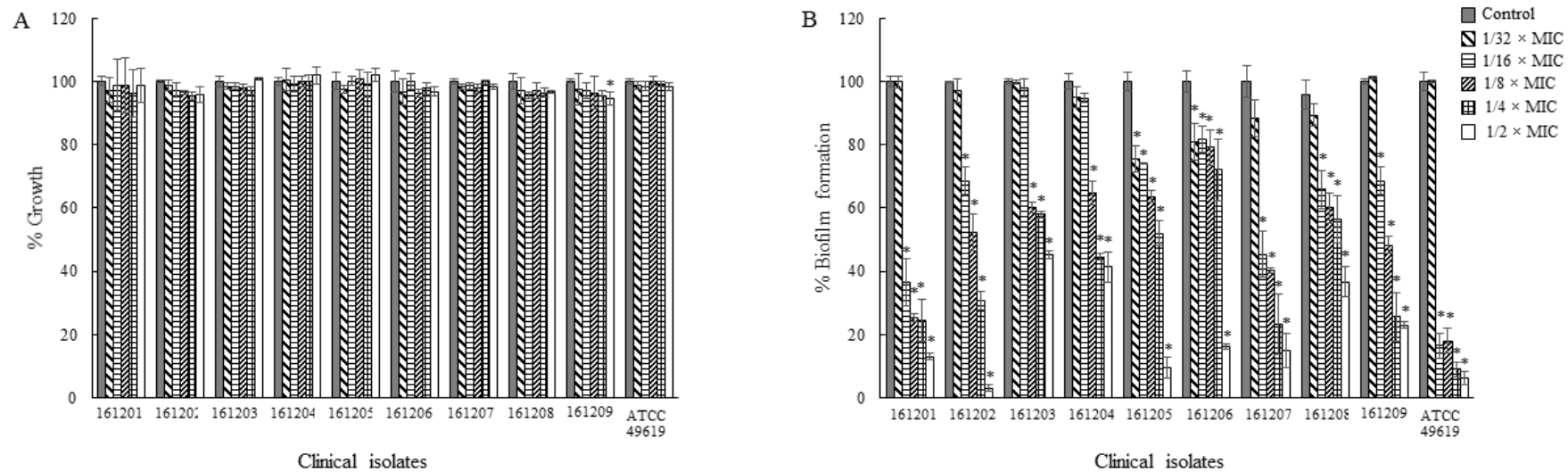


Figure 13. Effects of rhodomyrton on *Streptococcus pneumoniae* growth (A) and biofilm formation (B). The bacteria were cultured in the tested medium supplemented with rhodomyrton at sub-MICs. 1% DMSO was used as negative control. The relative percentage of biofilm formation was defined as: (mean A570 of treated well/mean A570 of control well) × 100, (* significant difference; $P < 0.05$).

3.9 Killing effects of *Rhodomyrtus tomentosa* ethanol extract and rhodomyrtone on pneumococcal established biofilm

Activity of the extract and rhodomyrtone on pneumococcal established biofilm was assessed by MTT assay. The viability of young (2-day-old-biofilm) and mature (8-day-old-biofilm) biofilm-grown cells significantly decreased following the treatment with the extract (Figure 14) and rhodomyrtone (Figure 15) at $16 \times \text{MIC}$.

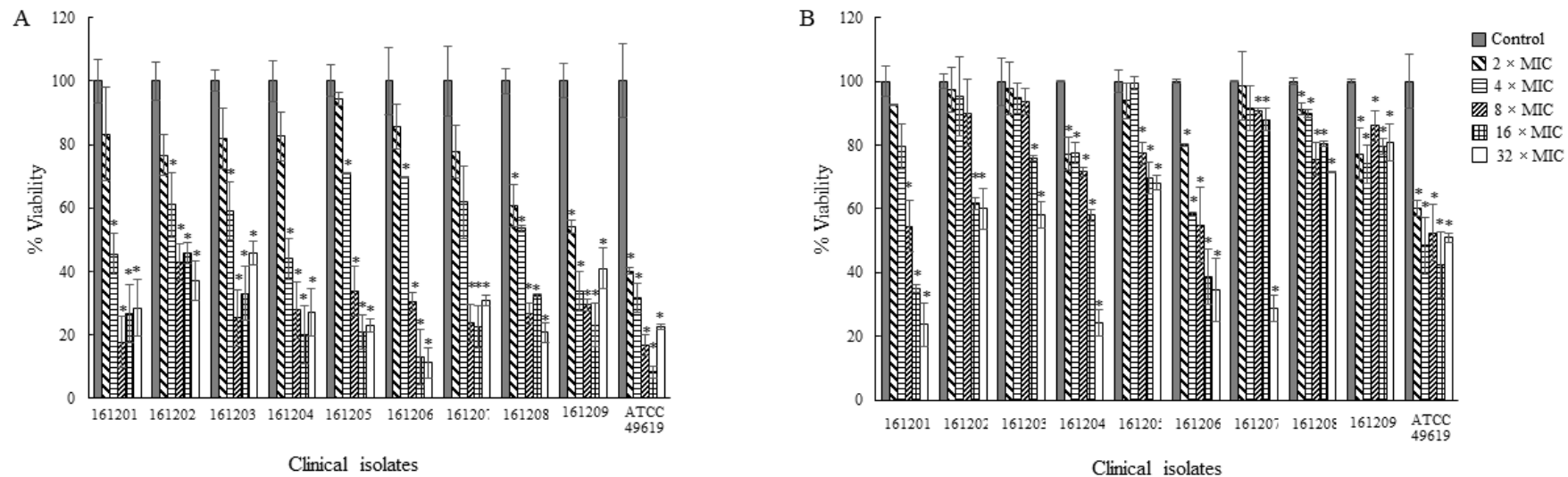


Figure 14. Inhibitory activity of *Rhodomyrtus tomentosa* ethanol extract on established biofilm of *Streptococcus pneumoniae*. The bacteria were cultured in MHB supplemented with 2.5% blood and 1% glucose to produce young (A) and mature (B) biofilms. The biofilms were then treated with *Rhodomyrtus tomentosa* extract at different concentrations. 1% DMSO was used as negative control. The relative percentage of biofilm viability was defined as: (mean A570 of treated well/mean A570 of control well) × 100, (* significant difference; $P < 0.05$).

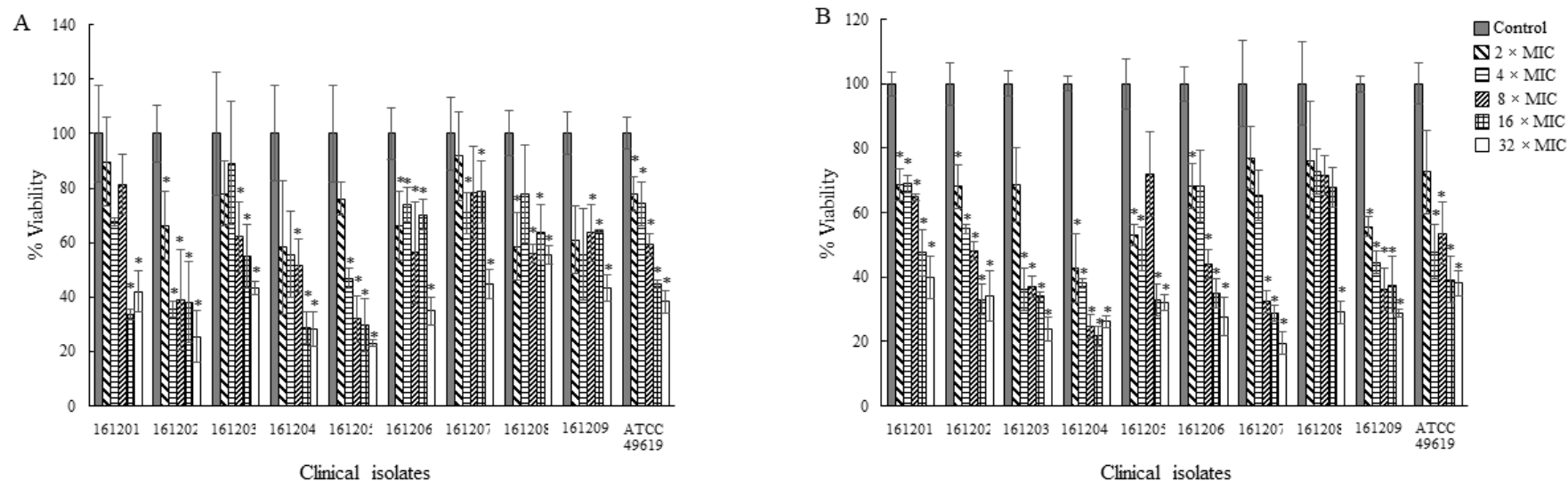


Figure 15. Inhibitory activity of rhodomlyrtone on established biofilm of *Streptococcus pneumoniae*. The bacteria were cultured in MHB supplemented with 2.5% blood and 1% glucose to produce young (A) and mature (B) biofilms. The biofilms were then treated with rhodomlyrtone at different concentrations. 1% DMSO was used as negative control. The relative percentage of biofilm viability was defined as: (mean A570 of treated well/mean A570 of control well) × 100, (* significant difference; $P < 0.05$).

3.10 Effects of *Rhodomyrtus tomentosa* extract and rhodomyrtone on pneumococcal adhesion and invasion to A549 human lung adenocarcinoma cell line

In order to apply *Rhodomyrtus tomentosa* extract and rhodomyrtone for the treatment of pneumococcal infections, effects of the extract and rhodomyrtone on invasiveness of pneumococci were further determined using A549 adenocarcinomic human alveolar basal epithelial cells. The extract and rhodomyrtone significantly inhibited pneumococcal adhesion to the epithelial cells ($P < 0.05$) (Figure 16A and 16B). At 30 min, 90% reduction in pneumococcal adhesion to the epithelial cells was detected (Figure 16A), while 40% reduction was observed in rhodomyrtone treated cells (Figure 16B). However, a longer time duration (90 min), approximately 70% reduction in the bacterial adhesion was detected following rhodomyrtone treatment.

Significant reduction in invasiveness of pneumococci to lung epithelial cells was detected following the treatment with the extract (Figure 17A) and rhodomyrtone (Figure 17B) at $1/2-1 \times \text{MIC}$, compared with the control ($P < 0.05$).

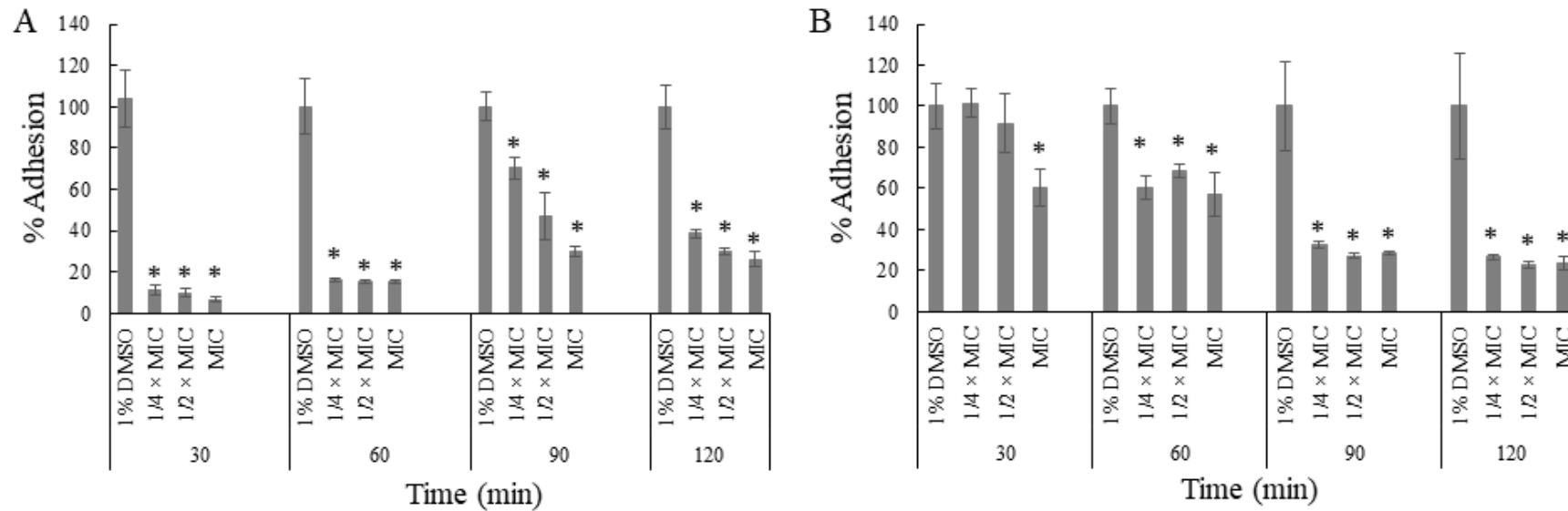


Figure 16. Effects of *Rhodomyrtus tomentosa* ethanol extract (A) and rhodomyrtone (B) on *Streptococcus pneumoniae* adhesion. The bacteria were cultured in the tested medium supplemented with the extract (MIC = 32 μ g/ml) and/or rhodomyrtone (MIC = 0.125 μ g/ml) at sub-MICs. 1% DMSO was used as negative control. The bacteria were incubated with A549 epithelial cells under 5% CO₂. Adhesive bacteria were counted on blood agar plates, and incubated at 37°C under 5% CO₂. Data are presented as a mean \pm SD.

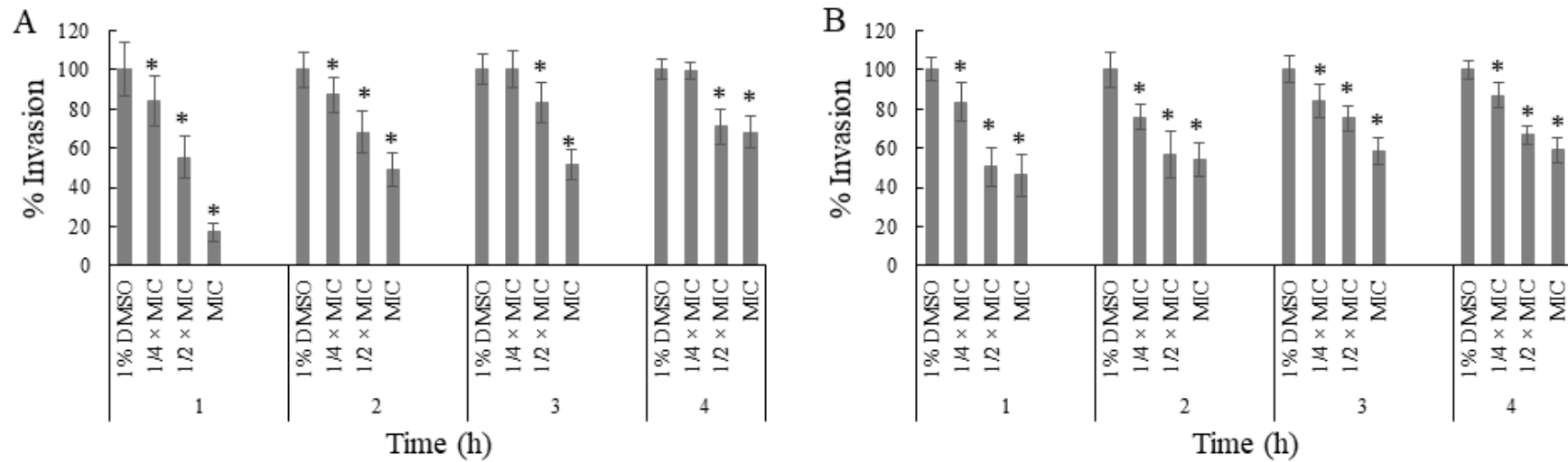


Figure 17. Effects of *Rhodomyrtus tomentosa* ethanol extract (A) and rhodomyrton (B) on *Streptococcus pneumoniae* invasion. The bacteria were cultured in the tested medium supplemented with the ethanol extract (MIC = 32 μ g/ml) and/or rhodomyrton (MIC = 0.125 μ g/ml) at different concentrations. 1% DMSO was used as negative control. The bacteria were incubated with A549 epithelial cells under 5% CO₂. Invasive bacteria were counted on blood agar plates, and incubated at 37°C under 5% CO₂. Data are presented as a mean \pm SD.

Chapter 4

Discussion

Infections caused by *S. pneumoniae* are an important cause of morbidity and mortality in humans including infants and older adults. The bacterium colonizes in the human upper respiratory tract including nasopharynx. Colonization is a prerequisite for subsequent spread, which may result in the infections. In the last decades, the spread of pneumococcal clones of the so-called “pediatric serotypes”, i.e. 6A, 6B, 9V, 14, 15A, 19A, 19F, and 23F has been reported (Cilloniz, Ardanuy et al. 2016). Actually, it is thought that antibiotic resistant selection occurs mainly in pneumococci colonizing young children, as they have high carriage rates and exposure to antibiotics, which favors the selection of drug resistance (Chao, Marks et al. 2014). However, selective pressure by vaccine-induced host immunity may also contribute to the appearance of new resistant strains, by increasing the frequency of serotypes with high non-susceptibility prevalence (Fenoll, Granizo et al. 2015).

It has been known for a long time that plants are a source of antimicrobial compounds (Mitrofanova, Yanitskaya et al. 2013). In this research, anti-pneumococcal activity of rhodomyrtone, an acylphloroglucinol compound isolated from *Rhodomyrtus tomentosa* leaves have studied. The results demonstrated that the extract and the compounds (both the purified and the synthetic ones) exhibited strong antibacterial activity against a collection of clinical isolates representative of the most prevalent serotypes. It is noted that the MIC values of rhodomyrtone for the clinical isolates was 64 times lower than that of the ethanol extract, which confirms it as an effective antimicrobial compound in the ethanol extract of *Rhodomyrtus tomentosa* leaves. Rhodomyrtone possessed pronounced antibacterial activity against the clinical isolates, even against those less susceptible to erythromycin, which might indicate differences in the mechanisms of action of both substances. Moreover, the ethanol extract and rhodomyrtone have a potential as a remarkable antibacterial agent to control a broad range of Gram-positive pathogens (Limsuwan, Trip et al. 2009, Saising, Ongsakul et al. 2011, Limsuwan, Kayser et al. 2012, Leejae, Taylor et al. 2013). This information indicated that rhodomyrtone presented a narrow-spectrum antibacterial

property with low levels of MIC and MBC. In addition, previous studies have shown that the purified compound did not produce toxic effects on human erythrocytes at a concentration of 128 µg/ml (Leejae, Taylor et al. 2013).

Rhodomyrton is originally isolated from *Rhodomyrton tomentosa* leaves (Salni, Sargent et al. 2002). However, rhodomyrton is now commercially available. Naturally purified rhodomyrton has been reported to be a small molecule. The molecular weight of the purified and synthetic rhodomyrton is 442.6 g/mole (Hiranrat and Mahabusarakam 2008) and 442.54 g/mole (Sigma), respectively. The present study revealed that both purified and synthetic rhodomyrton demonstrated a markedly pronounced antibacterial activity against the clinical isolates with similar MIC and MBC values. However, the MBC values of purified rhodomyrton for the reference strain was 4 times lower than that of the synthetic compound.

The Systems Biology era offers new opportunities to study global changes in microbes responding to any stimulus or stress, by means of the overview that the integration of different omic platforms provides (Fondi and Lio 2015, Pulido, Garcia-Quintanilla et al. 2016), which can be also applied to study the effect of antibiotics (Feng, Billal et al. 2011). In the present study, a multi-omics approach was applied to investigate the biological changes in *S. pneumoniae* in the presence of rhodomyrton.

metabolite profiles of the two studied pneumococcal reference strains exposed to rhodomyrton. The altered proteins were enzymes involved in important metabolic pathways. Proteomic analysis of cellular proteins demonstrated that proteins related to protein synthesis including cysteine synthase, ribosomal proteins and elongation factor Tu were reduced in response to the compound, as described for the effects of rhodomyrton on methicilin-resistant *S. aureus* (Sianglum, Srimanote et al. 2011). Furthermore, the compound also affected the amino acid synthesis. The levels of aspartic acid and tryptophan were reduced, while glutamic acid, tyrosine, and phenylalanine increased. Very interestingly, two enzymes of the arginine deiminase (ADI) pathway, i.e. arginine deiminase and ornithine carbamoyltransferase clearly decreased. The ADI pathway provides ATP in streptococcal species (Price, Zeyniyev et al. 2012). Recently, Allan et al have demonstrated the decrease in arginine deiminase

after nitric oxid treatment in the pneumococcus, an agent that causes dispersal in bacterial biofilms (Allan, Morgan et al. 2016). Moreover, deletion of the *arcD* gene, located at the ADI operon, impairs *S. pneumoniae* D39 capsule (Gupta, Yang et al. 2013). In addition, enzymes and metabolites involved in carbohydrate metabolism were strongly affected. Some enzymes of the glycolysis pathway were altered by rhodomyrtonone, as also observed in *S. pyogenes* (Limsuwan, Hesseling-Meinders et al. 2011). In the pneumococcus, the antimicrobial agent linezolid lead to alterations in glycolytic anzymes and lactate dehydrogenase in a similar way to what found in the present work (Feng, Billal et al. 2011). However, the Ru (II) complex X-03 caused also alterations in two glycolytic enzymes (6-PK and Eno) (Yang, Zhang et al. 2015), but just in opposite ways to what we have found in our study, thus suggesting possible differences in the mechanisms of action for the two antimicrobials. Two enzymes involved in the pyruvate metabolism, L-lactate dehydrogenase and acetate kinase, were diminished. It has been reported recently that these two enzymes are altered under oxidative stress (Lisher, Tsui et al. 2017), in a condition leading to a decrease in acetyl-CoA as we have found in this work. Also, there was a reduction of DNA gyrase A subunit. This enzyme is the target of quinolone antibiotics (Cilloniz, Ardanuy et al. 2016). The enzyme 3-oxoacyl-(acyl-carrier-protein) reductase, involved in fatty acid biosynthesis, was also reduced, as described for the antimicrobial agent Ru (II) complex X-03 (Yang, Zhang et al. 2015). In our view, the integrative proteomic and metabolomic analysis provided the key aspect of this research: rhodomyrtonone seems to affect pneumococcal capsule biosynthesis, as revealed by the observation that levels of two enzymes participating in the biosynthetic pathways, i.e. family-2 glycosyltransferase in R6 and UTP-glucose-1-phosphate uridylyltransferase (GalU) in TIGR4, and three metabolites, i.e. UDP-glucose (UDP-Glc), UDP-glucuronic acid (UDP-GlcUA) and UDP-N-acetyl-D-galactosamine (UDP-GalpNAc), clearly diminished. Glycosyltransferases catalyze the assembly of the repeating units of the capsular polysaccharide by transferring of sugar residues from the appropriate sugar donor, i.e. a sugar phosphate, to an activated lipid carrier on the cytoplasmic face of the cell membrane (Oliver, van der Linden et al. 2013, Shainheit, Valentino et al. 2015). R6 is a non-encapsulated type-2 strain derived from the encapsulated, virulent D39 strain. R6 lacks a 7,504-bp region of the D39 genome coding for 7 out of the 9 genes

(*SPD_0315* through *SPD_0323*) in a cluster responsible for the capsule biosynthesis (Iannelli, Pearce et al. 1999, Hoskins, Alborn et al. 2001). However, as in other strains, R6 possesses other loci in the genome annotated as functions participating in exopolysaccharide/capsule synthesis/glycosyltransferase activity which are out of the previously cited cluster region: *spr0091* and *spr0092* code for sugar transferase related protein and capsule polysaccharide biosynthesis protein CapD, respectively; *spr1654* and *spr1655* code for a capsular polysaccharide biosynthesis protein and a glycosyltransferase, respectively; and *spr0135* and *spr0136* code for an exopolysaccharide (EPS) synthesis glycosyltransferase and a glycosyltransferase, family 2, respectively. Whether this last gene product could have a role in the synthesis of type 2 capsule remains unknown, as R6 lacks the genes for capsule formation and, to our knowledge, its function has not been studied so far.

GalU catalyzes the formation of UDP-Glc, which is the substrate for the synthesis of UDP-GlcUA (Mollerach, Lopez et al. 1998), carried out by the enzyme UDP-glucose dehydrogenase (Aanensen, Mavroidi et al. 2007). UDP-GlcUA plays a central role in the formation of many microbial capsules, including those of *S. pyogenes*, *E.coli* K5, and *Cryptococcus neoformans*, as well as of many *S. pneumoniae* serotypes (Ventura, Cartee et al. 2006). We tested the effect of the compound at sub-MICs on pneumococcal capsule formation on 8 clinical isolates of *S. pneumoniae* representing 8 serotypes, some of them coinciding with the so-called “pediatric isolates”; i.e. we selected representative isolates of the most prevalent isolates in pediatric patients. Rhodomyrtone-treated pneumococcal cells significantly possessed less amount of capsule, when compared with untreated cells. All the tested isolates were affected, including that of serotype 3. This serotype has a mechanism of capsule biosynthesis different to that of the other serotypes (Ventura, Cartee et al. 2006). However, our data revealed that serotype-3 capsule was reduced in the same extension as for the other serotypes. Whether both biosynthesis pathway types are equally affected or not was beyond the objective of this work. Very recently, it has been described that pneumococcal capsule production by strains harboring capsules with acetylated sugars, as for TIGR4, depends on the presence of pyruvate oxidase, and that a type-4 background mutant lacking this enzyme also had much lower levels of acetyl-CoA,

suggesting that capsule reduction/loss arises from dysregulation of this crucial metabolite (Echlin, Frank et al. 2016). Pyruvate oxidase converts pyruvate to acetyl-phosphate, which can be converted to acetate via acetate kinase or to acetyl-CoA via phosphate acetyltransferase. Also very recently, it has been reported that a decrease in acetate kinase is correlated to lower acetyl-CoA levels (Lisher, Tsui et al. 2017). Therefore, our findings of decreased abundances in both acetate kinase and acetyl-CoA are in agreement with these recently published results.

In addition, other proteins and metabolites may be affected rather than those identified in our analysis, but the fact that using 2-D gels of total cell extract may have masked minor differences that might be present, but undetectable. A question arising from this research is whether the pneumococcal virulence is reduced after rhodomyrtone treatment. We could not see differences in the abundances of virulence factors such as pneumolysin or neuraminidase, but the use of other more sensitive proteomic approaches, rather than 2-D gels, could help to this aim. Further research using mutants in different pneumococcal serotypes will be needed further resolve the mechanism of action of rhodomyrtone and to study its possible implication in pneumococcal colonization/adherence.

The results demonstrated that expression of two enzymes (glycosyltransferase and galU) and three metabolites (UDP-Glc, UDP-Glc-UA and UDP-N-acetyl-D-galactosamine) involved in the synthesis of pneumococcal capsule was suppressed upon exposure to rhodomyrtone. It was observed that rhodomyrtone-treated pneumococcal cells significantly possessed less amount of capsule when compared with the untreated cells. Capsule polysaccharide of *S. pneumoniae* plays a role against phagocytosis. It was found that significant increase in phagocytosis of pneumococci was observed when the bacteria were treated with sub-MICs of the extract and rhodomyrtone, compared with the control. It may suggest that inhibition of pneumococcal capsule formation by rhodomyrtone could enhance bacterial phagocytosis by the macrophages.

The potential of *Rhodomyrtus tomentosa* extract and rhodomyrtone as inhibitors against *S. pneumoniae* biofilm formation was further investigated. The results revealed that the extract and rhodomyrtone significantly inhibited pneumococcal

biofilm formation. It was observed that growth of the isolates was significantly inhibited by the extract at $1/4$ and $1/2 \times$ MIC. This may be due to other compounds present in the extract (Liu, Tan et al. 2016). Similarly, activity of the extract and rhodomyrtone against *S. aureus* (Saising, Ongsakul et al. 2011) and *S. pyogenes* (Limsuwan and Voravuthikunchai 2008) biofilms has been reported by our research group. The mechanisms of plant derived compounds on biofilm inhibition may involve in the inhibition of aggregation and buildup of biofilm (Yadav, Park et al. 2013), inhibition of bacterial quorum sensing system (Limsuwan and Voravuthikunchai 2008, Reen, Gutiérrez-Barranquero et al. 2018) as well as killing due to their excellent antimicrobial activity (Kwieciński, Eick et al. 2009). Previous study reported anti-quorum sensing activity of *Rhodomyrtus tomentosa* extract on a biomonitor strain, *Chromobacterium violaceum*, resulting in the inhibition of violacein pigment production (Limsuwan and Voravuthikunchai 2008). Quorum sensing regulates the biofilm by production and sensing of pheromone called autoinducer. It has been reported that Rgg/ small hydrophobic peptide (SHP) quorum-sensing systems are widespread in streptococci including *S. pneumoniae* (Junges, Salvadori et al. 2017). It has been reported that an expression of both *shp* and *rgg* genes increased at the stationary growth phase of *S. pneumoniae* (Junges, Salvadori et al. 2017). The present study observed the biofilm inhibition at the stationary growth phase. Moreover, the study on proteomic and metabolomic analysis of *S. pneumoniae* treated with rhodomyrtone revealed that rhodomyrtone suppressed proteins involved in biofilms including cysteine synthase. The protein was found to be over expressed in *S. pneumoniae* biofilm (Allan, Skipp et al. 2014).

The viability of young and mature biofilm-grown cells significantly decreased following the treatment with the extract and rhodomyrtone. Arginine deiminase system protects bacterial cells against damaging effects of acid environments (Casiano-Colón and Marquis 1988). Carbohydrate fermentation by bacteria embedded in the biofilm generates acidic metabolites. Arginine deiminase generates L-citrulline and ammonia from L-arginine. The produced ammonia could neutralize acid metabolites in the biofilms. Therefore, arginine deiminase activity could be important in protection against the acid in biofilm maturation. The present study demonstrated

that rhodomyrtone suppressed arginine deiminase expression as revealed by proteomic analysis. In this study, MHB supplemented with 1% glucose was used as tested medium to investigate effects of rhodomyrtone on pneumococcal biofilm. Glucose was added as substrate for biofilm formation. It has been documented that the medium supplemented with 1% glucose showed high biofilm formation, when compared with the control (Yadav, Chae et al. 2012). However, it has been reported that arginine deiminase expression is subjected to carbon catabolism repression (Dong, Chen et al. 2004). Supplementation of glucose and L-arginine in the growth medium significantly increased the activity of arginine deiminase (Wang and Li 2014).

In order to apply *Rhodomyrtus tomentosa* extract and rhodomyrtone for the treatment of pneumococcal infections, effects of the extract and rhodomyrtone on invasiveness of pneumococci were further determined using A549 adenocarcinomic human alveolar basal epithelial cells. The extract and rhodomyrtone significantly inhibited pneumococcal adhesion and invasion to the epithelial cells. Similarly, *S. aureus* treated with the extract and rhodomyrtone showed a reduction in their adhesion to human buccal cells (Limsuwan, Homlaead et al. 2014) and invasiveness in bovine udder epidermal tissue (Mordmuang, Shankar et al. 2015). This may due to down-regulation of pneumococcal glyceraldehyde-3-phosphate dehydrogenase (Mitsuwan, Olaya-Abril et al. 2017). This protein is an important glycolytic enzyme which involves various functions including adhesion and invasion (Barbosa, Bao et al. 2006). It was noted that the extract showed better anti-adhesive activity than rhodomyrtone at 30 min. Several tannin is presented in *Rhodomyrtus tomentosa* leaves (Liu, Hou et al. 1998). The mode of action of tannin may interfere with microbial adhesins, enzymes, and cell envelope transport proteins (Cowan 1999).

Pneumococcus is an endemic global pathogen that causes a wide range of disease in children and adults. The bacterium is one of the most important pathogens in otitis media. It has been reported that *S. pneumoniae* serotype 19A ST320 is the predominant cause of pneumococcal mastoiditis, a suppurative complication of acute otitis media (Chi, Chiu et al. 2018). The present study demonstrated that rhodomyrtone possessed antibacterial activity against the clinical isolates of pneumococci including

the serotype 19A. Moreover, the pure compound at sub-MICs inhibited the capsule polysaccharide produced by the isolate.

The findings reveal the utility of combining proteomic and metabolomic analyses to provide insight into phenotypic features of *S. pneumoniae* treated with rhodomyrtone. The results suggested potential medicinal benefits of the extract and rhodomyrtone for inhibiting of the pathogen. This can lead to an alternative antibiotic for the treatment of *S. pneumoniae* infections.

Chapter 5

Conclusion

The integration of different omics is a powerful tool to shed light into key pathways that can be altered by a given experimental condition. This work provides insight into the effect of rhodomyrtone, a non-conventional antimicrobial compound, on the pneumococcus at molecular level, by means of integrating proteomics and metabolomics. The data indicated, among other alterations, a reduction of enzymes (glycosyltransferase and galU) and metabolites (UDP-Glc, UDP-Glc-UA and UDP-N-acetyl-D-galactosamine) involved in the capsule biosynthesis. These findings indicate that rhodomyrtone has a potential as antibacterial therapy and could be used in the future if resistance to conventional antibiotics used to treat pneumococcal infections emerge significantly. In addition, our study shows the utility of multi-omic approaches to describe the molecular effects of drugs on pathogenic bacteria.

The present study supports pronounced effects of *Rhodomyrtus tomentosa* extract and rhodomyrtone on the Gram-positive pathogen. Both the extract and rhodomyrtone inhibited pneumococcal biofilm formation and eradicated established biofilm in *S. pneumoniae*. The extract and rhodomyrtone significantly reduced pneumococcal adhesion and invasion to A549 human lung adenocarcinoma cell line. Increase in phagocytosis of the bacterial cells by RAW264.7 macrophage cell line was observed following the treatment with the extract and rhodomyrtone, compared with the control. The results suggested potential medicinal benefits of the extract and rhodomyrtone for the treatment of pneumococcal infections.

In conclusion, rhodomyrtone is a promising alternative antibacterial agent for the treatment of the infections caused by the Gram-positive pathogens including *S. pneumoniae*.

REFERENCES

- Aanensen, D. M., A. Mavroidi, S. D. Bentley, P. R. Reeves and B. G. Spratt. 2007. Predicted functions and linkage specificities of the products of the *Streptococcus pneumoniae* capsular biosynthetic loci. *Journal of Bacteriology* 189(21): 7856-7876.
- Abdeldaim, G. M., K. Strålin, P. Olcén, J. Blomberg, and B. Herrmann. 2008. Toward a quantitative DNA-based definition of pneumococcal pneumonia: a comparison of *Streptococcus pneumoniae* target genes, with special reference to the Spn9802 fragment. *Diagnostic Microbiology and Infectious Disease* 60(2): 143-150.
- Akhtar, M. S. and V. Bhakuni. 2003. *Streptococcus pneumoniae* Hyaluronate Lyase Contains Two Non-cooperative Independent Folding/Unfolding Structural Domains characterization of functional domain and inhibitors of enzyme. *Journal of Biological Chemistry* 278(28): 25509-25516.
- Akhtar, M. S. and V. Bhakuni. 2004. *Streptococcus pneumoniae* hyaluronate lyase: An overview. *Current Science*: 285-295.
- Allan, R. N., S. Morgan, S. Brito-Mutunayagam, P. Skipp, M. Feelisch, S. M. Hayes, W. Hellier, S. C. Clarke, P. Stoodley, A. Burgess, H. Ismail-Koch, R. J. Salib, J. S. Webb, S. N. Faust and L. Hall-Stoodley. 2016. Low Concentrations of Nitric Oxide Modulate *Streptococcus pneumoniae* Biofilm Metabolism and Antibiotic Tolerance. *Antimicrobial Agents and Chemotherapy* 60(4): 2456-2466.
- Allan, R. N., P. Skipp, J. Jefferies, S. C. Clarke, S. N. Faust, L. Hall-Stoodley and J. Webb. 2014. Pronounced metabolic changes in adaptation to biofilm growth by *Streptococcus pneumoniae*. *PLoS One* 9(9): e107015.
- Barbosa, M. S., S. N. Bão, P. F. Andreotti, F. P. de Faria, M. S. S. Felipe, L. dos Santos Feitosa, M. J. S. Mendes-Giannini and C. M. de Almeida Soares. 2006. Glyceraldehyde-3-phosphate dehydrogenase of *Paracoccidioides*

brasiliensis is a cell surface protein involved in fungal adhesion to extracellular matrix proteins and interaction with cells. *Infection and Immunity* 74(1): 382-389.

- Baril, L., J. Dietemann, M. Essevaz-Roulet, L. Beniguel, P. Coan, D. Briles, B. Guy and G. Cozon. 2006. Pneumococcal surface protein A (PspA) is effective at eliciting T cell-mediated responses during invasive pneumococcal disease in adults. *Clinical and Experimental Immunology* 145(2): 277-286.
- Barocchi, M., J. Ries, X. Zogaj, C. Hemsley, B. Albiger, A. Kanth, S. Dahlberg, J. Fernebro, M. Moschioni and V. Massignani. 2006. A pneumococcal pilus influences virulence and host inflammatory responses. *Proceedings of the National Academy of Sciences* 103(8): 2857-2862.
- Boulware, D. R., C. L. Daley, C. Merrifield, P. C. Hopewell and E. N. Janoff. 2007. Rapid diagnosis of pneumococcal pneumonia among HIV-infected adults with urine antigen detection. *Journal of Infection* 55(4): 300-309.
- Brooks-Walter, A., D. E. Briles and S. K. Hollingshead. 1999. The *pspC* gene of *Streptococcus pneumoniae* encodes a polymorphic protein, PspC, which elicits cross-reactive antibodies to PspA and provides immunity to pneumococcal bacteremia. *Infection and Immunity* 67(12): 6533-6542.
- Cai, K., Y. Wang, Z. Guo, X. Xu, H. Li and Q. Zhang. 2018. Clinical characteristics and antimicrobial resistance of pneumococcal isolates of pediatric invasive pneumococcal disease in China. *Infection and Drug Resistance* 11: 2461.
- Casiano-Colón, A. and R. E. Marquis. 1988. Role of the arginine deiminase system in protecting oral bacteria and an enzymatic basis for acid tolerance. *Applied and Environmental Microbiology* 54(6): 1318-1324.
- Chao, Y., L. R. Marks, M. M. Pettigrew and A. P. Hakansson. 2015. *Streptococcus pneumoniae* biofilm formation and dispersion during colonization and disease. *Frontiers in Cellular and Infection Microbiology* 4: 194.

- Charpentier, E. and E. Tuomanen. 2000. Mechanisms of antibiotic resistance and tolerance in *Streptococcus pneumoniae*. *Microbes and Infection* 2(15): 1855-1864.
- Chi, H., N.-C. Chiu, F.-Y. Huang, C.-H. Hsu, K.-s. Lee, L.-M. Huang and Y.-C. Hsieh. 2018. Acute otitis media caused by *Streptococcus pneumoniae* serotype 19A ST320 clone: epidemiological and clinical characteristics. *Journal of Microbiology, Immunology and Infection* 51(3): 337-343.
- Chorachoo, J., T. Amnuait and S. P. Voravuthikunchai. 2013. Liposomal encapsulated rhodomyrtone: a novel antiacne drug. *Evidence-Based Complementary and Alternative Medicine* 2013. 157635.
- Chorachoo, J., S. Lambert, T. Furnholm, L. Roberts, L. Reingold, S. Auepemkiate, S. P. Voravuthikunchai, and A. Johnston. 2018) The small molecule rhodomyrtone suppresses TNF- α and IL-17A-induced keratinocyte inflammatory responses: A potential new therapeutic for psoriasis. *PloS One* 13(10): e0205340.
- Chorachoo, J., D. Saeloh, T. Srichana, T. Amnuait, K. S. Musthafa, S. Sretrirutchai and S. P. Voravuthikunchai. 2016. Rhodomyrtone as a potential anti-proliferative and apoptosis inducing agent in HaCaT keratinocyte cells. *European Journal of Pharmacology* 772: 144-151.
- Cillóniz, C., C. García-Vidal, A. Moreno, J. M. Miro and A. Torres. 2018. Community-acquired bacterial pneumonia in adult HIV-infected patients. *Expert review of Anti-Infective Therapy* 16(7): 579-588.
- Cowan, M. M. 1999. Plant products as antimicrobial agents. *Clinical Microbiology Reviews* 12(4): 564-582.
- Domenech, M., E. Ramos-Sevillano, E. García, M. Moscoso and J. Yuste. 2013. Biofilm formation avoids complement immunity and phagocytosis of *Streptococcus pneumoniae*. *Infection and Immunity* 81(7): 2606-2615.

- Dong, Y., Y.-Y. M. Chen, and R. Burne. 2004. Control of expression of the arginine deiminase operon of *Streptococcus gordonii* by CcpA and Flp. *Journal of Bacteriology* 186(8): 2511-2514.
- Echlin, H., M. W. Frank, A. Iverson, T. C. Chang, M. D. Johnson, C. O. Rock and J. W. Rosch. 2016. Pyruvate Oxidase as a Critical Link between Metabolism and Capsule Biosynthesis in *Streptococcus pneumoniae*. *PLoS Pathogens* 12(10): e1005951.
- Farooqui, H., M. Jit, D. L. Heymann and S. Zodpey. 2015. Burden of severe pneumonia, pneumococcal pneumonia and pneumonia deaths in Indian states: modelling based estimates. *PloS One* 10(6): e0129191.
- Feng, J., D. S. Billal, A. Lupien, G. Racine, E. Winstall, D. Legare, P. Leprohon and M. Ouellette. 2011. Proteomic and transcriptomic analysis of linezolid resistance in *Streptococcus pneumoniae*. *Journal of Proteome Research* 10(10): 4439-4452.
- Fenoll, A., J. J. Granizo, M. J. Gimenez, J. Yuste and L. Aguilar. 2015. Secular trends (1990-2013) in serotypes and associated non-susceptibility of *S. pneumoniae* isolates causing invasive disease in the pre-/post-era of pneumococcal conjugate vaccines in Spanish regions without universal paediatric pneumococcal vaccination. *Vaccine* 33(42): 5691-5699.
- Fondi, M. and P. Lio. 2015. Multi -omics and metabolic modelling pipelines: challenges and tools for systems microbiology. *Microbiological Research* 171: 52-64.
- Geno, K. A., G. L. Gilbert, J. Y. Song, I. C. Skovsted, K. P. Klugman, C. Jones, H. B. Konradsen and M. H. Nahm. 2015. Pneumococcal capsules and their types: past, present, and future. *Clinical Microbiology Reviews* 28(3): 871-899.
- Gillespie, S. and I. Balakrishnan. 2000. Pathogenesis of pneumococcal infection. *Journal of Medical Microbiology* 49(12): 1057-1067.
- Gor, D. O., X. Ding, Q. Li, D. Sultana, S. S. Mambula, R. J. Bram and N. S. Greenspan. 2011. Enhanced immunogenicity of pneumococcal surface

adhesin A (PsaA) in mice via fusion to recombinant human B lymphocyte stimulator (BLyS). *Biology Direct* 6(1): 9.

Gupta, R., J. Yang, Y. Dong, E. Swiatlo, J. R. Zhang, D. W. Metzger and G. Bai. 2013. Deletion of *arcD* in *Streptococcus pneumoniae* D39 impairs its capsule and attenuates virulence. *Infection and Immunity* 81(10): 3903-3911.

Hathaway, L. J., D. Grandgirard, L. G. Valente, M. G. Täuber and S. L. Leib. 2016. *Streptococcus pneumoniae* capsule determines disease severity in experimental pneumococcal meningitis. *Open Biology* 6(3): 150269.

Hiranrat, A. and W. Mahabusarakam 2008. New acylphloroglucinols from the leaves of *Rhodomyrtus tomentosa*. *Tetrahedron* 64(49): 11193-11197.

Hirst, R. A., B. Gosai, A. Rutman, C. J. Guerin, P. Nicotera, P. W. Andrew and C. O'callaghan. 2008. *Streptococcus pneumoniae* deficient in pneumolysin or autolysin has reduced virulence in meningitis. *The Journal of Infectious Diseases* 197(5): 744-751.

Hoskins, J., W. E. Alborn, Jr., J. Arnold, L. C. Blaszcak, S. Burgett, B. S. DeHoff, S. T. Estrem, L. Fritz, D. J. Fu, W. Fuller, C. Geringer, R. Gilmour, J. S. Glass, H. Khoja, A. R. Kraft, R. E. Lagace, D. J. LeBlanc, L. N. Lee, E. J. Lefkowitz, J. Lu, P. Matsushima, S. M. McAhren, M. McHenney, K. McLeaster, C. W. Mundy, T. I. Nicas, F. H. Norris, M. O'Gara, R. B. Peery, G. T. Robertson, P. Rokey, P. M. Sun, M. E. Winkler, Y. Yang, M. Young-Bellido, G. Zhao, C. A. Zook, R. H. Baltz, S. R. Jaskunas, P. R. Rosteck, Jr., P. L. Skatrud and J. I. Glass. 2001. Genome of the bacterium *Streptococcus pneumoniae* strain R6. *Journal of Bacteriology* 183(19): 5709-5717.

Hyams, C., E. Camberlein, J. M. Cohen, K. Bax and J. S. Brown. 2010. The *Streptococcus pneumoniae* capsule inhibits complement activity and neutrophil phagocytosis by multiple mechanisms. *Infection and Immunity* 78(2): 704-715.

Iannelli, F., B. J. Pearce and G. Pozzi. 1999. The type 2 capsule locus of *Streptococcus pneumoniae*. *Journal of Bacteriology* 181(8): 2652-2654.

- Iovino, F., D. L. Hammarlöf, G. Garriss, S. Brovall, P. Nannapaneni and B. Henriques-Normark. 2016. Pneumococcal meningitis is promoted by single cocci expressing pilus adhesin RrgA. *The Journal of Clinical Investigation* 126(8): 2821-2826.
- James, D. B., K. Gupta, J. R. Hauser and J. Yother. 2013. Biochemical activities of *Streptococcus pneumoniae* serotype 2 capsular glycosyltransferases and significance of suppressor mutations affecting the initiating glycosyltransferase Cps2E. *Journal of Bacteriology* 195(24): 5469-5478.
- Jumbe, N. L., A. Louie, M. H. Miller, W. Liu, M. R. Deziel, V. H. Tam, R. Bachhawat and G. L. Drusano. 2006. Quinolone efflux pumps play a central role in emergence of fluoroquinolone resistance in *Streptococcus pneumoniae*. *Antimicrobial Agents and Chemotherapy* 50(1): 310-317.
- Junges, R., G. Salvadori, S. Shekhar, H. A. Åmdal, J. N. Periselneris, T. Chen, J. S. Brown and F. C. Petersen. 2017. A Quorum-Sensing System that regulates *Streptococcus pneumoniae* biofilm formation and surface polysaccharide production. *mSphere* 2(5): e00324-00317.
- Knippenberg, S., B. Ueberberg, R. Maus, J. Bohling, N. Ding, M. T. Tarres, H.-G. Hoymann, D. Jonigk, N. Izykowski and J. C. Paton. 2015. *Streptococcus pneumoniae* triggers progression of pulmonary fibrosis through pneumolysin. *Thorax* 70(7): 636-646.
- Korona-Glowniak, I., P. Zychowski, R. Siwiec, E. Mazur, G. Niedzielska and A. Malm. 2018. Resistant *Streptococcus pneumoniae* strains in children with acute otitis media—high risk of persistent colonization after treatment. *BMC Infectious Diseases* 18(1): 478.
- Kurola, P., L. Erkkilä, T. Kaijalainen, A. A. Palmu, W. P. Hausdorff, J. Poolman, J. Jokinen, T. M. Kilpi, M. Leinonen and A. Saukkoriipi. 2010. Presence of capsular locus genes in immunochemically identified encapsulated and unencapsulated *Streptococcus pneumoniae* sputum isolates obtained from

- elderly patients with acute lower respiratory tract infection. *Journal of Medical Microbiology* 59(10): 1140-1145.
- Kwieciński, J., S. Eick and K. Wójcik. 2009. Effects of tea tree (*Melaleuca alternifolia*) oil on *Staphylococcus aureus* in biofilms and stationary growth phase. *International Journal of Antimicrobial Agents* 33(4): 343-347.
- Lai, T. N. H., M.-F. Herent, J. Quetin-Leclercq, T. B. T. Nguyen, H. Rogez, Y. Larondelle and C. M. André. 2013. Piceatannol, a potent bioactive stilbene, as major phenolic component in *Rhodomyrtus tomentosa*. *Food Chemistry* 138(2-3): 1421-1430.
- Lee, M. S., J. Y. Oh, C.-I. Kang, E. S. Kim, S. Park, C. K. Rhee, J. Y. Jung, K.-W. Jo, E. Y. Heo, and D.-A. Park. 2018. Guideline for antibiotic use in adults with community-acquired pneumonia. *Infection and Chemotherapy* 50(2): 160-198.
- Leejae, S., P. W. Taylor and S. P. Voravuthikunchai. 2013. Antibacterial mechanisms of rhodomyrtone against important hospital-acquired antibiotic-resistant pathogenic bacteria. *Journal of Medical Microbiology* 62(1): 78-85.
- Leejae, S., B.-e. Yingyongnarongkul, A. Suksamrarn and S. P. Voravuthikunchai. 2012. Synthesis and structure–activity relationship of rhodomyrtone derivatives as antibacterial agent. *Chinese Chemical Letters* 23(9): 1011-1014.
- Limsuwan, S., A. Hesselting-Meinders, S. P. Voravuthikunchai, J. M. van Dijn and O. Kayser. 2011. Potential antibiotic and anti-infective effects of rhodomyrtone from *Rhodomyrtus tomentosa* (Aiton) Hassk. on *Streptococcus pyogenes* as revealed by proteomics. *Phytomedicine* 18(11): 934-940.
- Limsuwan, S., S. Homlaead, S. Watcharakul, S. Chusri, K. Moosigapong, J. Saising and S. P. Voravuthikunchai. 2014. Inhibition of microbial adhesion to plastic surface and human buccal epithelial cells by *Rhodomyrtus tomentosa* leaf extract. *Archives of Oral Biology* 59(12): 1256-1265.
- Limsuwan, S., O. Kayser and S. P. Voravuthikunchai. 2012. Antibacterial activity of *Rhodomyrtus tomentosa* (Aiton) Hassk. leaf extract against clinical

isolates of *Streptococcus pyogenes*. Evidence-Based Complementary and Alternative Medicine 2012: 697183.

Limsuwan, S., E. N. Trip, T. R. Kouwen, S. Piersma, A. Hiranrat, W. Mahabusarakam, S. P. Voravuthikunchai, J. M. van Dijn and O. Kayser. 2009. Rhodomyrtone: a new candidate as natural antibacterial drug from *Rhodomyrtus tomentosa*. Phytomedicine 16(6-7): 645-651.

Limsuwan, S. and S. P. Voravuthikunchai. 2008. *Boesenbergia pandurata* (Roxb.) Schltr., *Eleutherine americana* Merr. and *Rhodomyrtus tomentosa* (Aiton) Hassk. as antibiofilm producing and antiquorum sensing in *Streptococcus pyogenes*. FEMS Immunology and Medical Microbiology 53(3): 429-436.

Lisher, J. P., H. T. Tsui, S. Ramos-Montanez, K. L. Hentchel, J. E. Martin, J. C. Trinidad, M. E. Winkler and D. P. Giedroc. 2017. Biological and chemical adaptation to endogenous hydrogen peroxide production in *Streptococcus pneumoniae* D39. mSphere 2(1): e00291-16.

Liu, H.-X., K. Chen, Y. Yuan, Z.-F. Xu, H.-B. Tan and S.-X. Qiu. 2016. Rhodomentones A and B, novel meroterpenoids with unique NMR characteristics from *Rhodomyrtus tomentosa*. Organic and Biomolecular Chemistry 14(30): 7354-7360.

Liu, H.-X., H.-B. Tan and S.-X. Qiu. 2016. Antimicrobial acylphloroglucinols from the leaves of *Rhodomyrtus tomentosa*. Journal of Asian Natural Products Research 18(6): 535-541.

Liu, H.-X., W.-M. Zhang, Z.-F. Xu, Y.-C. Chen, H.-B. Tan and S.-X. Qiu. 2016. Isolation, synthesis, and biological activity of tomentosenol A from the leaves of *Rhodomyrtus tomentosa*. RSC Advances 6(31): 25882-25886.

Liu, J., J.-G. Song, J.-C. Su, X.-J. Huang, W.-C. Ye and Y. Wang (2018). "Tomentodione E, a new sec-pentyl syncarpic acid-based meroterpenoid from the leaves of *Rhodomyrtus tomentosa*." Journal of Asian Natural Products Research 20(1): 67-74.

- Liu, Y., A. Hou, C. Ji and Y. Wu. 1998. Isolation and structure of hydrolysable tannins from *Rhodomyrtus tomentosa*. *Natural Product Research and Development* 10(1): 14-19.
- Mandell, L. A., R. G. Wunderink, A. Anzueto, J. G. Bartlett, G. D. Campbell, N. C. Dean, S. F. Dowell, T. M. File Jr, D. M. Musher and M. S. Niederman. 2007. Infectious Diseases Society of America/American Thoracic Society consensus guidelines on the management of community-acquired pneumonia in adults. *Clinical Infectious Diseases* 44(Supplement 2): S27-S72.
- Marion, C., J. M. Stewart, M. F. Tazi, A. M. Burnaugh, C. M. Linke, S. A. Woodiga and S. J. King. 2012. *Streptococcus pneumoniae* can utilize multiple sources of hyaluronic acid for growth. *Infection and Immunity* 80(4): 1390-1398.
- Martner, A., C. Dahlgren, J. C. Paton and A. E. Wold. 2008. Pneumolysin released during *Streptococcus pneumoniae* autolysis is a potent activator of intracellular oxygen radical production in neutrophils. *Infection and Immunity* 76(9): 4079-4087.
- Mayoral, C., M. B. Della, M. Baroni, R. Giani, M. Regueira and F. Zalazar. 2010. Pneumococcal surface protein A (PspA) families. Relation with serotypes and clinical site of infection. *Medicina* 70(5): 437-441.
- Mellroth, P., R. Daniels, A. Eberhardt, D. Rönnlund, H. Blom, J. Widengren, S. Normark and B. Henriques-Normark. 2012. LytA, major autolysin of *Streptococcus pneumoniae*, requires access to nascent peptidoglycan. *Journal of Biological Chemistry* 287(14): 11018-11029.
- Mitrofanova, I. Y., A. V. Yanitskaya and D. V. Butenko 2013. Methodological aspects of optimizing the choice of plants for creation of new drugs. *Bulletin of Experimental Biology and Medicine* 155(5): 647-649.
- Mitsuwan, W., A. Olaya-Abril, M. Calderón-Santiago, I. Jiménez-Munguía, J. A. González-Reyes, F. Priego-Capote, S. P. Voravuthikunchai and M. J. Rodríguez-Ortega. 2017. Integrated proteomic and metabolomic analysis

reveals that rhodomyrtone reduces the capsule in *Streptococcus pneumoniae*.X Scientific Reports 7(1): 2715.

- Mollerach, M., R. Lopez and E. Garcia. 1998. Characterization of the galU gene of *Streptococcus pneumoniae* encoding a uridine diphosphoglucose pyrophosphorylase: a gene essential for capsular polysaccharide biosynthesis. Journal of Experimental Medicine 188(11): 2047-2056.
- Mordmuang, A., S. Shankar and S. P. Voravuthikunchai. 2015. Effects of *Rhodomyrtus tomentosa* leaf extract on staphylococcal adhesion and invasion in bovine udder epidermal tissue model. Nutrients 7(10): 8503-8517.
- Moreno, A. T., M. L. S. Oliveira, P. L. Ho, C. F. Vadesilho, G. M. Palma, J. M. Ferreira, D. M. Ferreira, S. R. Santos, M. B. Martinez and E. N. Miyaji. 2012. Cross-reactivity of antipneumococcal surface protein C (PspC) antibodies with different strains and evaluation of inhibition of human complement factor H and secretory IgA binding via PspC. Clinical and Vaccine Immunology 19(4): 499-507.
- Na-Phatthalung, P., M. Teles, S. P. Voravuthikunchai, L. Tort and C. Fierro-Castro. 2018. Immunomodulatory effects of *Rhodomyrtus tomentosa* leaf extract and its derivative compound, rhodomyrtone, on head kidney macrophages of rainbow trout (*Oncorhynchus mykiss*). Fish Physiology and Biochemistry 44(2): 543-555.
- Niederman, M. S., L. A. Mandell, A. Anzueto, J. B. Bass, W. A. Broughton, G. D. Campbell, N. Dean, T. File, M. J. Fine and P. A. Gross. 2001. Guidelines for the management of adults with community-acquired pneumonia: diagnosis, assessment of severity, antimicrobial therapy, and prevention. American Journal of Respiratory and Critical Care Medicine 163(7): 1730-1754.
- Odedina, G. F., K. Vongkamjan and S. P. Voravuthikunchai. 2016. Use of *Rhodomyrtus tomentosa* ethanolic leaf extract for the bio-control of *Listeria monocytogenes* post-cooking contamination in cooked chicken meat. Journal of Food Science and Technology 53(12): 4234-4243.

- Oliveira, M. L. S., E. N. Miyaji, D. M. Ferreira, A. T. Moreno, P. C. Ferreira, F. A. Lima, F. L. Santos, M. A. Sakauchi, C. S. Takata and H. G. Higashi. 2010. Combination of pneumococcal surface protein A (PspA) with whole cell pertussis vaccine increases protection against pneumococcal challenge in mice. *PLoS One* 5(5): e10863.
- Oliver, M. B., M. P. van der Linden, S. A. Kuntzel, J. S. Saad and M. H. Nahm. 2013. Discovery of *Streptococcus pneumoniae* serotype 6 variants with glycosyltransferases synthesizing two differing repeating units. *The Journal of Biological Chemistry* 288(36): 25976-25985.
- Pancotto, L., G. De Angelis, E. Bizzarri, M. A. Barocchi, G. Del Giudice, M. Moschioni and P. Ruggiero. 2013. Expression of the *Streptococcus pneumoniae* pilus-1 undergoes on and off switching during colonization in mice. *Scientific Reports* 3: 2040.
- Patel, S. N., A. McGeer, R. Melano, G. J. Tyrrell, K. Green, D. R. Pillai, D. E. Low and C. B. S. Network. 2011. Susceptibility of *Streptococcus pneumoniae* to fluoroquinolones in Canada. *Antimicrobial Agents and Chemotherapy* 55(8): 3703-3708.
- Peppoloni, S., B. Colombari, R. Neglia, D. Quaglino, F. Iannelli, M. R. Oggioni, G. Pozzi and E. Blasi. 2006. The lack of pneumococcal surface protein C (PspC) increases the susceptibility of *Streptococcus pneumoniae* to the killing by microglia. *Medical Microbiology and Immunology* 195(1): 21-28.
- Peppoloni, S., S. Ricci, C. F. Orsi, B. Colombari, M. M. De Santi, M. Messinò, G. Fabio, A. Zanardi, E. Righi and V. Braione. 2010. The encapsulated strain TIGR4 of *Streptococcus pneumoniae* is phagocytosed but is resistant to intracellular killing by mouse microglia. *Microbes and Infection* 12(12-13): 990-1001.
- Price, C. E., A. Zeyniyev, O. P. Kuipers and J. Kok. 2012. From meadows to milk to mucosa-adaptation of *Streptococcus* and *Lactococcus* species to their nutritional environments. *FEMS Microbiology Reviews* 36(5): 949-971.

- Pulido, M. R., M. Garcia-Quintanilla, M. L. Gil-Marques and M. J. McConnell. 2016. Identifying targets for antibiotic development using omics technologies. *Drug Discov Today* 21(3): 465-472.
- Quin, L. R., C. Onwubiko, Q. C. Moore, M. F. Mills, L. S. McDaniel and S. Carmicle. 2007. Factor H binding to PspC of *Streptococcus pneumoniae* increases adherence to human cell lines in vitro and enhances invasion of mouse lungs in vivo. *Infection and Immunity* 75(8): 4082-4087.
- Rai, P., F. He, J. Kwang, B. P. Engelward and V. T. Chow. 2016. Pneumococcal pneumolysin induces DNA damage and cell cycle arrest. *Scientific Reports* 6: 22972.
- Rajam, G., J. M. Anderton, G. M. Carlone, J. S. Sampson and E. W. Ades. 2008. Pneumococcal surface adhesin A (PsaA): a review. *Critical Reviews in Microbiology* 34(3-4): 131-142.
- Reen, F. J., J. A. Gutiérrez-Barranquero and M. L. Parages. 2018. Coumarin: a novel player in microbial quorum sensing and biofilm formation inhibition. *Applied Microbiology and Biotechnology* 102(5): 2063-2073.
- Saeloh, D., V. Tipmanee, K. K. Jim, M. P. Dekker, W. Bitter, S. P. Voravuthikunchai, M. Wenzel and L. W. Hamoen. 2018. The novel antibiotic rhodomyrtone traps membrane proteins in vesicles with increased fluidity. *PLoS Pathogens* 14(2): e1006876.
- Saising, J., M. Ongsakul and S. P. Voravuthikunchai. 2011. *Rhodomyrtus tomentosa* (Aiton) Hassk. ethanol extract and rhodomyrtone: a potential strategy for the treatment of biofilm-forming staphylococci. *Journal of Medical Microbiology* 60(12): 1793-1800.
- Saising, J. and S. P. Voravuthikunchai. 2012. Anti *Propionibacterium acnes* activity of rhodomyrtone, an effective compound from *Rhodomyrtus tomentosa* (Aiton) Hassk. leaves. *Anaerobe* 18(4): 400-404.

- Salni, D., M. V. Sargent, B. W. Skelton, I. Soediro, M. Sutisna, A. H. White and E. Yulinah. 2002. Rhodomyrtone, an antibiotic from *Rhodomyrtus tomentosa*. *Australian Journal of Chemistry* 55(3): 229-232.
- Sato, T., K. Tateda, S. Kimura, M. Iwata, Y. Ishii and K. Yamaguchi. 2011. In vitro antibacterial activity of modithromycin, a novel 6, 11-bridged bicyclicolide, against respiratory pathogens, including macrolide-resistant Gram-positive cocci. *Antimicrobial Agents and Chemotherapy* 55(4): 1588-1593.
- Schachern, P. A., V. Tsuprun, P. Ferrieri, D. E. Briles, S. Goetz, S. Cureoglu, M. M. Paparella and S. Juhn. 2014. Pneumococcal PspA and PspC proteins: potential vaccine candidates for experimental otitis media. *International Journal of Pediatric Otorhinolaryngology* 78(9): 1517-1521.
- Seo, J.-Y., S. Y. Seong, B.-Y. Ahn, I. C. Kwon, H. Chung and S. Y. Jeong. 2002. Cross-protective immunity of mice induced by oral immunization with pneumococcal surface adhesin a encapsulated in microspheres. *Infection and Immunity* 70(3): 1143-1149.
- Shainheit, M. G., M. D. Valentino, M. S. Gilmore and A. Camilli. 2015. Mutations in pneumococcal *cpsE* generated via in vitro serial passaging reveal a potential mechanism of reduced encapsulation utilized by a conjunctival isolate. *Journal of Bacteriology* 197(10): 1781-1791.
- Sianglum, W., P. Srimanote, P. W. Taylor, H. Rosado and S. P. Voravuthikunchai. 2012. Transcriptome analysis of responses to rhodomyrtone in methicillin-resistant *Staphylococcus aureus*. *PloS One* 7(9): e45744.
- Sianglum, W., P. Srimanote, W. Wonglumsom, K. Kittiniyom and S. P. Voravuthikunchai (2011). Proteome analyses of cellular proteins in methicillin-resistant *Staphylococcus aureus* treated with rhodomyrtone, a novel antibiotic candidate. *PLoS One* 6(2): e16628.
- Solano, C., M. Echeverez, and I. Lasa. 2014. Biofilm dispersion and quorum sensing. *Current opinion in microbiology* 18: 96-104.

- Srisuwan, S., P. Tongtawe, P. Srimanote and S. P. Voravuthikunchai (2014). Rhodomyrtone modulates innate immune responses of THP-1 monocytes to assist in clearing methicillin-resistant *Staphylococcus aureus*. PloS one 9(10): e110321.
- Surve, M. V., S. Bhutda, A. Datey, A. Anil, S. Rawat, A. Pushpakaran, D. Singh, K. S. Kim, D. Chakravorty and A. Banerjee. 2018. Heterogeneity in pneumolysin expression governs the fate of *Streptococcus pneumoniae* during blood-brain barrier trafficking. PLoS Pathogens 14(7): e1007168.
- Taha, N., G. F. Araj, R. H. Wakim, S. S. Kanj, Z. A. Kanafani, A. Sabra, M.-T. Khairallah, F. J. Nassar, M. Shehab and M. Baroud. 2012) Genotypes and serotype distribution of macrolide resistant invasive and non-invasive *Streptococcus pneumoniae* isolates from Lebanon. Annals of Clinical Microbiology and Antimicrobials 11(1): 2.
- Tseng, H.-J., A. G. McEwan, J. C. Paton and M. P. Jennings. 2002. Virulence of *Streptococcus pneumoniae*: PsaA mutants are hypersensitive to oxidative stress. Infection and Immunity 70(3): 1635-1639.
- van der Poll, T. and S. M. Opal. 2009. Pathogenesis, treatment, and prevention of pneumococcal pneumonia. The Lancet 374(9700): 1543-1556.
- Ventura, C. L., R. T. Cartee, W. T. Forsee and J. Yother. 2006. Control of capsular polysaccharide chain length by UDP-sugar substrate concentrations in *Streptococcus pneumoniae*. Molecular Microbiology 61(3): 723-733.
- Voravuthikunchai, S. P., S. Dolah, and W. Chareernjiratrakul. 2010. Control of *Bacillus* compound. Journal of food protection 73(10): 1907-1912.
- Wai-Haan, H. and L. Man-Moon. 1976. Two new triterpenoids from *Rhodomyrtus tomentosa*. Phytochemistry 15(11): 1741-1743.
- Wang, Y. and Y.-Z. Li. 2014. Cultivation to improve in vivo solubility of overexpressed arginine deiminases in *Escherichia coli* and the enzyme characteristics. BMC biotechnology 14(1): 53.

- Wen, Z., Y. Liu, F. Qu and J. R. Zhang. 2016. Allelic variation of the capsule promoter diversifies encapsulation and virulence in *Streptococcus pneumoniae*. *Scientific Reports* 6: 30176.
- Wu, K., H. Xu, Y. Zheng, L. Wang, X. Zhang and Y. Yin. 2016. CpsR, a GntR family regulator, transcriptionally regulates capsular polysaccharide biosynthesis and governs bacterial virulence in *Streptococcus pneumoniae*. *Scientific Reports* 6: 29255.
- Yadav, M. K., S.-W. Chae and J.-J. Song. 2012) In vitro *Streptococcus pneumoniae* biofilm formation and in vivo middle ear mucosal biofilm in a rat model of acute otitis induced by *S. pneumoniae*. *Clinical and Experimental Otorhinolaryngology* 5(3): 139.
- Yadav, M. K., S. W. Park, S. W. Chae, J. J. Song and H. C. Kim. 2013. Antimicrobial activities of *Eugenia caryophyllata* extract and its major chemical constituent eugenol against *Streptococcus pneumoniae*. *Apmis* 121(12): 1198-1206.
- Yang, X. Y., L. Zhang, J. Liu, N. Li, G. Yu, K. Cao, J. Han, G. Zeng, Y. Pan, X. Sun and Q. Y. He. 2015. Proteomic analysis on the antibacterial activity of a Ru(II) complex against *Streptococcus pneumoniae*. *Journal of Proteomics* 115: 107-116.
- Yother, J. 2011. Capsules of *Streptococcus pneumoniae* and other bacteria: paradigms for polysaccharide biosynthesis and regulation. *Annual Review of Microbiology* 65: 563-581.
- Yuste, J., M. Botto, J. C. Paton, D. W. Holden and J. S. Brown. 2005. Additive inhibition of complement deposition by pneumolysin and PspA facilitates *Streptococcus pneumoniae* septicemia. *The Journal of Immunology* 175(3): 1813-1819.
- Zhang, J.-R., K. E. Mostov, M. E. Lamm, M. Nanno, S.-i. Shimida, M. Ohwaki and E. Tuomanen. 2000. The polymeric immunoglobulin receptor translocates

pneumococci across human nasopharyngeal epithelial cells. *Cell* 102(6): 827-837.

Zhang, Y.-L., C. Chen, X.-B. Wang, L. Wu, M.-H. Yang, J. Luo, C. Zhang, H.-B. Sun, J.-G. Luo, and L.-Y. Kong. 2016. "Rhodomyrtals A and B, two meroterpenoids with a triketone-sesquiterpene-triketone skeleton from *Rhodomyrtus tomentosa*: structural elucidation and biomimetic synthesis." *Organic Letters* 18(16): 4068-4071.

Zivich, P. N., J. D. Grabenstein, S. I. Becker-Dreps and D. J. Weber. 2018. *Streptococcus pneumoniae* outbreaks and implications for transmission and control: a systematic review. *Pneumonia* 10(1): 11.

VITAE

Name Mr. Watcharapong Mitsuwan

Student ID 5410230009

Educational Attainment

Degree	Name of Institution	Year of Graduation
B.Sc. (Microbiology) (1 st Class Honors)	Prince of Songkla University	2011

Scholarship Awards during Enrolment

2011-2015 Royal Golden Jubilee (RGJ) Ph.D. Program Scholarship,
grant number; PHD/0053/2553, The Thailand Research Fund, Thailand

List of Publication

Mitsuwan, W., Olaya-Abril, A., Calderón-Santiago, M., Jiménez-Munguía, I., González-Reyes, J.A., Priego-Capote, F., Voravuthikunchai S.P. and Rodríguez-Ortega, M.J. Integrated proteomic and metabolomic analysis reveals that rhodomyrton reduces the capsule in *Streptococcus pneumoniae*. Scientific Reports. 2017; 7: 2715.

Mitsuwan, W., Jiménez-Munguía, I., Visutthi, M., Sianglum, W., REIPI/GEIH Study Group, Rodríguez-Ortega, M.J. and Voravuthikunchai, S.P. Rhodomyrton decreases *Staphylococcus aureus* SigB activity during exponentially growing phase and inhibits haemolytic activity within membrane vesicles. Microbial Pathogenesis. 2019; 112-118.

Mitsuwan, W., Wintachai, P., and Voravuthikunchai, S.P. *Rhodomyrtus tomentosa* leaf extract and rhodomyrtone combat *Streptococcus pneumoniae* biofilm and inhibit invasiveness to human lung epithelial and enhance pneumococcal phagocytosis by macrophage. Microbial Pathogenesis (submitted).

List of Poster Presentation

Mitsuwan, W., Chusri, S and Voravuthikunchai, S.P. 2012. Thai medicinal plant extracts as resistant modifying agent against multidrug resistant Gram-negative bacteria. The Fourth International Conference on Natural Products for Health and Beauty. 28th-30th November 2012, Chiang Mai, Thailand.

Mitsuwan, W., Voravuthikunchai, S.P, Olaya-Abril, A., Gonzales Reyes, J.A., Jimenez-Munguia, I. and Rodriguez-Ortega, M.J. 2014. Sub-inhibitory rhodomyrtone concentration reduces *Streptococcus pneumoniae* capsule production. The 5th International Conference on Natural Products for Health and Beauty. 6th -8th May 2014. Phuket. Thailand.

Mitsuwan, W., Vorvuthikunchai, S.P., Jiménez-Munguía, I., Olaya-Abril, A. and Rodríguez-Ortega, M.J. 2015. Pronounced antibacterial activity of rhodomyrtone against *Streptococcus pneumoniae* as revealed by proteomic analysis. 113th TRF Seminar Series in Basic Research “From Basic Research to Application”. 25th September 2015, Seminar Room, Faculty of Science, Prince of Songkla University, Thailand.

Mitsuwan, W., Musthafa, K.S., Vorvuthikunchai, S.P. 2016. *Rhodomyrtus tomentosa* (Aiton) Hassk extract: potential as anti-biofilm agent against *Streptococcus pneumoniae*. The 6th International Conference on Natural Products for Health and Beauty (NATPRO6). 21st-23rd January 2016, Pullman Raja Orchid Hotel, Khon Kaen, Thailand.

Mitsuwan, W., Vorvuthikunchai, S.P., Jiménez-Munguía, I., Olaya-Abril, A., and Rodríguez-Ortega, M. 2016. Responses in the expression of proteins in *Streptococcus pneumoniae* treated with rhodomyrtone as revealed by proteomic

analysis. RGJ – Ph.D. Congress 17. 8th -11th June 2016, Jomtien Palm Beach Hotel and Resort, Pattaya, Chonburi, Thailand.

Mitsuwan, W., Wintachai, P., and Voravuthikunchai, S.P. 2017. Effects of *Rhodomyrtus tomentosa* leaf extract on *Streptococcus pneumoniae* adhesion and invasion to human alveolar epithelial cell line A549. UKM-UR-UII-PSU Joint Seminar 2017. 20th - 22th November 2017. Marriott Hotel and Universiti Kebangsaan Malaysia. Malaysia.

Mitsuwan, W and Voravuthikunchai, S.P. *Rhodomyrtus tomentosa* (Aiton) Hassk. leaf extract and rhodomyrtone: potential anti-virulence agents against *Streptococcus pneumoniae*. The 7th International Conference on Natural Products. 18th-20th October 2018, Hotel Hyundai, Gyeongju, Korea.